Metamaterials and Metasurfaces for Wireless Power Transfer and Energy Harvesting

Jiafeng Zhou, *Senior Member, IEEE*, Pei Zhang, Jiaqi Han, Long Li, *Senior Member, IEEE*, and Yi Huang, *Fellow, IEEE*

***Abstract*— A comprehensive review of metamaterials and metasurfaces for wireless power transfer (WPT) and wireless energy harvesting (WEH) is presented in this paper. According to the features of the electromagnetic field from the source to the receiver, WPT is divided into non-radiative near-field technology and radiative (near and far-field) technologies. Many different and important designs are reviewed and compared. It is shown that metamaterials and metasurfaces can significantly improve the power transfer efficiency and operational distance for WPT systems. They can also improve the energy conversion efficiency of wireless energy harvesters by making the reception less sensitive to incident wave angle and polarization. A rectenna is a critical element for both WPT and WEH. It is shown that metamaterial-based rectennas can achieve a higher RF to DC conversion efficiency. Furthermore, metamaterials can also be used as either parasitic elements or loading components to improve WEH performance in terms of circuit size, beamwidth, and conversion efficiency. Future development directions and opportunities of metamaterials and metasurfaces for WPT and WEH are also proposed in this paper.**

***Index Terms*—Antennas, metamaterials, metasurfaces, rectennas, wireless energy harvesting, wireless power transfer.**

I. Introduction

WIRELESS has become an essential feature of many modern technologies and systems. The 5th generation (5G) of mobile radio communications and the Internet of Things (IoT) are just two well-known wireless examples. Wireless power transfer (WPT) and wireless energy harvesting (WEH) using electromagnetic (EM) waves are two less well-known examples, but they are becoming increasingly important for the wireless industry. Unlike a wired system, which is good for a point-to-point connection, a wireless system can offer connectivity from a point to a large area, and provide convenience and flexibility.

WPT has been introduced for wireless charging for such as mobile phones and electric vehicles where charging cables can be avoided [1]-[4]. Significant progress has been made over the past 20 years. Although near field coupling is at the moment the dominant approach in applications, far-field WPT is also in high demand [1], [2].

WEH is similar to WPT but with the focus on converting the received EM energy from the environment to power low-power IoT devices, to avoid battery replacement [5]-[7]. Thus, unlike the WPT, WEH is for a much lower power level and possibly operates across a broad frequency band. The power harvested is typically less than 1 μW which is not enough for most practical applications, but it is envisaged that the power consumption of many IoT devices will continue to fall while the harvested energy will be increased, thus, the future of WEH seems to be bright.

A major problem for both WPT and WEH is the low RF-DC (radio frequency to direct current) energy conversion efficiency. The signal from the RF source is first received by an antenna or a coil at RF frequencies and then rectified to a DC voltage/current as DC energy for applications. This energy conversion efficiency is affected by such as the polarization mismatch, sensitivity to wave incident angle, misalignment, impedance mismatch, and nonlinearity of the rectifying circuit. How to increase this efficiency is a very hot and challenging topic.

Metamaterials and metasurfaces have been introduced to realize some special functions which cannot be obtained using normal natural materials. They have found a wide range of applications [8], [9]. One of them is for WPT and WEH. There have been very interesting research activities and results, but the information is relatively scattered and patched, there is a lack of a good overview of this subject. The objective of this paper is therefore to provide a comprehensive review on how metamaterials and metasurfaces have been used for WPT and WEH from the near-field and far-field, two different approaches. The focus is on WPT.

Metamaterials and metasurfaces are introduced in Section II. The aim is to provide a good understanding of these new materials. The general overview of WPT and WEH is introduced in Section III. Section IV is to discuss how to use

This work was supported in part by the EPSRC (UK), in part by National Key R&D Program of China and in part by Royal Society (UK) (*The corresponding author is Yi Huang*).

J. F. Zhou and Y. Huang are with the Department of Electrical Engineering and Electronics at the University of Liverpool, Liverpool, L69 3GJ, UK (e-mail: Jiafeng.Zhou, Yi.Huang@Liverpool.ac.uk).

P. Zhang, J. Han, and L. Li are with the Key Laboratory of High Speed Circuit Design and EMC, Ministry of Education, School of Electronic Engineering, Xidian University, Xi'an 710071, China (e-mail: 805514773@qq.com, jqhan@xidian.edu.cn, lilong@mail.xidian.edu.cn).

.

metamaterials and metasurfaces for non-radiative near-field WPT, while Section V is to address how to employ metamaterials and metasurfaces for radiative near and far-field WPT and WEH. The discussion is provided and future developments are proposed in Section VI. Conclusions are drawn in Section VII.

II. Metamaterials and Metasurfaces

The prefix *meta* is a Greek word and means "beyond, about", thus a metamaterial indicates that the characteristics of the material are beyond what we see in nature. Metamaterials are artificially crafted composite materials that derive their properties from internal microstructure, rather than chemical composition found in natural materials. The concept might have been introduced a long time ago [8], but the realization and applications have been just about 20 years [10]-[14]. The interest has been growing significantly over the last decade or so since this new type of material has a wide range of potential applications from low microwave to optical frequencies[15], [16]. There are a number of commercial applications in the market related to metamaterials, for example, the metamaterial-enabled design of antennas for space applications [17]. Metamaterials have been used in radomes and radar systems in general for many years [18]. Metamaterial-based antennas and antenna arrays are widely available [19][20]. Recently they have been engineered for 5G and autonomous vehicle applications [21]. Emerging applications of metamaterials include non-invasive glucose sensing, proprietary metasurfaces for magnetic resonance imaging machines and radio wave imaging [22] [23]. One very notable product related to the topic of this paper is a metaboard using metamaterials made of coupled resonant elements for wireless charging [24].

The core concept of metamaterials is to produce materials by using artificially designed and fabricated structural units made of metallic or dielectric materials to achieve the desired properties and functionalities. These sub-wavelength structural units – the constituent artificial 'atoms' and 'molecules' of the metamaterial – can be tailored in shape and size. The lattice constant and interatomic interaction can be artificially tuned. They can be designed and placed at desired locations. By engineering the arrangement of these small unit cells into a desired architecture or geometry, one can tune the effective permittivity or permeability of the metamaterial to positive, near-zero, or negative values. Thus, metamaterials can be endowed with properties and functionalities unattainable in natural materials [11], [12].

Fig. 1 shows that materials can be divided into four categories according to their effective permittivity ε and permeability μ [25]:

1) Conventional double-positive (DPS) materials: both of their permittivity ε and permeability μ are positive which are what we find in the natural world.

2) Epsilon-negative (ENG) materials: they display a negative permittivity ε but positive permeability μ. ENG could be formed using conducting rods (thin wires). In this case, the refractive index becomes imaginary, and EM waves cannot propagate in the material but reflected at the boundary between air and the medium. Any propagation into the medium would be evanescent.

3) Mu-negative (MNG) materials: they have a positive ε but negative μ. MNG and could be formed using split-ring resonators (SRRs). Again, in this case, the refractive index becomes imaginary and EM waves cannot propagate in the material and will be reflected at the boundary between air and the material.

4) Double negative (DNG) materials: both the permittivity ε and permeability μ are negative. DNG could be formed using conducting rods and SRRs. EM waves at the boundary between air and the medium are partially reflected and partially refracted into the medium in different directions compared with that for a DPS material as shown in Fig. 1. In this case, the refraction index n becomes negative, EM waves travel in the backward direction in the medium. The phenomenon is new and not observed in natural materials. Both the reflection and refraction are anomalous, and Snell's law does not work in this case. DNG metamaterials are sometimes termed "left-handed materials (LHM)" due to the left-handedness of the electric field, the magnetic field, and the wave vector.

Strictly speaking, a material with an effective relative permittivity positive but less than 1, and/or an effective relative permeability positive but less than 1, can also be called a metamaterial. Thus, another property that cannot normally be found in nature but can be achieved with metamaterials is that of a near-zero refractive index. This could be Epsilon near zero (ENZ) or Mu near-zero (MNZ) materials as indicated in Figure 1. Occasionally, a material with a positive, but extremely high, permittivity or permeability is also be called a metamaterial.

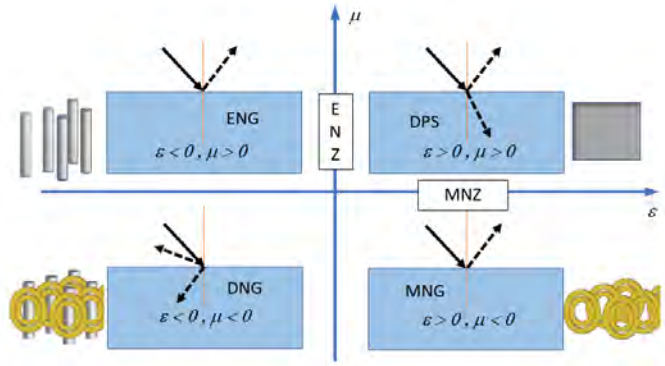

Fig. 1. Material classification [25]

The metamaterials in general are composite materials. Each unit cell (SRR or other designs) has an individually tailored response to the EM field. This is similar to how light interacts with everyday materials; materials such as glass or lenses are made of atoms. An averaging or macroscopic effect is produced. The cell of a metamaterial is designed to mimic the EM response of atoms, only on a much larger scale. Also, as part of periodic composite structures, these are designed to have a stronger EM coupling than is found in nature. The larger scale allows for more control over the EM response, while each unit is smaller than the wavelength of the radiated EM wave.

To achieve fascinating functionalities of metamaterials typically entails multiple stacks of material layers, which not only leads to extensive loss but also brings a lot of challenges in fabrication. Many metamaterials consist of complex metallic wires and other structures that require sophisticated fabrication technology and are difficult to assemble. Three-dimensional

(3D) metamaterials can be extended by arranging electrically small scatters or holes into a two-dimensional (2D) pattern at a surface or interface. This surface version of a metamaterial has been given the name ***metasurface***. For many applications, metasurfaces can be used in place of metamaterials. They have the advantage of taking up less physical space than full 3D metamaterial structures do; consequently, they offer the possibility of less-lossy structures as well. Thus, metasurfaces have attracted greater attention than 3D metamaterials and advanced very rapidly over the past ten years or so.

Over the years, there have been many special periodic surface structures developed, such as the frequency selective surface (FSS), high impedance surface (HIS), and EM bandgap (EBG) structures. An important question is: Are they metasurfaces?

These special structures are named after their specific functions or macroscopic performances while metamaterials and metasurfaces are defined by the bulk material properties: realized effective permittivity and permeability. Thus, they are named from different levels: one is from the material level while the other is from the function level. That is why metasurfaces usually overlap with many research areas of conventional 2D periodic structures. For example, frequency selective surfaces [26], [27] can be implemented using metasurfaces, not metamaterials, depending on the specific design. Generally speaking, the conventional frequency selective surface is not a metamaterial, but high impedance surfaces and EM bandgap structures are normally considered as metamaterials.

III. WPT AND WEH

In a typical WPT system, a transmitter (Tx) device generates a time-varying EM field and transmits power across space to a receiver (Rx) device. Since the EM field from an RF/microwave source can be divided into non-radiative near-field, radiative near-field (Fresnel) field, and radiative far-field, WPT can be roughly divided into two categories: non-radiative (near-field), and radiative (near and far-field) techniques.

For the non-radiative WPT, the energy is transmitted through electric field or magnetic field coupling which is called capacitive or inductive coupling, respectively. They can be further divided into resonant and non-resonant coupling as shown in Fig. 2 [28]. In this case, power is transferred over short distances, usually within one wavelength from the Tx. It is often operated at low frequencies (kHz up to about 30 MHz). Inductive coupling is the most common approach because it is relatively easy to implement high inductance (hence high power) at lower frequencies although capacitive coupling can be useful in some applications where sufficient space is available for big capacitive plates (and high power) [29].

For inductive coupling, power is transferred between coils of wire by a magnetic field. Resonant inductive coupling is a form of inductive coupling in which power is transferred by magnetic fields between two resonant circuits, one in the Tx and another in the Rx. By using resonance, power can be transferred at greater distances with higher flexibility. Another advantage is that resonant circuits interact with each other much more strongly than they do with other objects. Most commercially available wireless charging devices (e.g. electric vehicles) use this technique.

For the radiative WPT, the energy can be transferred through the radiative near-field or the far-field of the source where the power is inversely proportional to the distance square. In this case, power is transferred through waves at high frequencies (above 30 MHz) usually. It is more suitable for long-distance (more than a wavelength) applications. The system could be divided into microwave WPT and laser WPT. Currently, the main activities are in microwave WPT due to its low cost and easy accessibility.

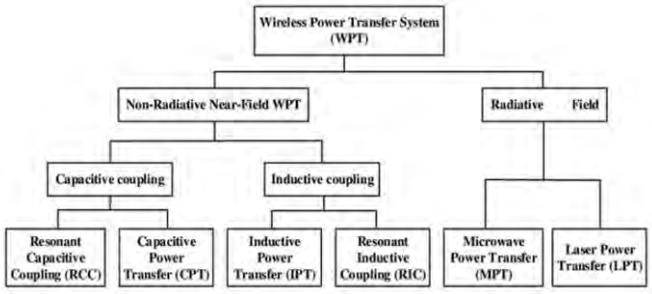

Fig. 2. Classification of WPT based on [28]

The main difference between the non-radiative and radiative WPT systems is reflected by their EM energy transmitting and receiving devices: coils are normally used for the former while antennas are employed for the latter. But their Tx and Rx circuits are very similar. They all employ the same key device, called ***rectenna*** (rectifying antenna). The block diagram of a rectenna is given in Fig. 3 where the antenna could be a coil at low frequencies. The EM energy received by the antenna will be rectified to DC which can then be stored or used in applications. This device has been heavily studied over the years [6], [30], [31]. Many good designs are available although there is still room for improvement.

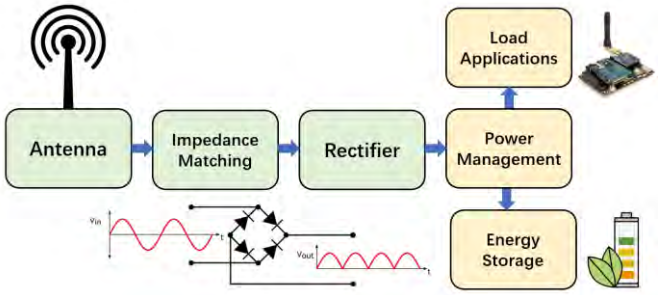

Fig. 3. Block diagram of a rectenna for wireless power transfer and energy harvesting.

A WEH system could be considered as the receiving part of a WPT system (i.e. the rectenna) since the WPT consists of both the Tx and Rx while WEH is mainly about the Rx. But there are many differences.

WPT is often for high-power applications. It is point-to-point and polarization-aligned. It operates over a narrowband, requiring antennas of good directivity. In WPT applications, metamaterials/metasurfaces were introduced to tailor the wavefront based on the amplitude/phase regulation characteristics of the metasurface elements.

On the other hand, WEH mainly harvests ambient RF energy and is space-to-point, normally requiring an omnidirectional antenna pattern with a wide beamwidth (or wide-angle), ideally insensitive to the incident angle. Ambient RF power discretely distributes in different communication bands from hundreds of MHz to several GHz. It suggests that a WEH harvester should have wideband or multi-band characteristics. Furthermore, ambient EM waves are often accompanied by different polarizations, requiring WEH harvesters to have polarization-insensitive characteristics, also called polarization-angle independent characteristics in some literature. Additionally, WEH harvesters should possess the structural characteristics of planarization, low-profile, and miniaturization since the application terminals are often low-power sensors.

A comprehensive comparison between them will be given in Section V.

A common problem for WPT and WEH is how to improve the energy conversion efficiency which is a complex issue. It is linked to the antenna or coil performance (efficiency, bandwidth, polarization, and orientation), impedance matching, non-linearity of the rectifier, and power management. The use of metamaterials and metasurfaces can help improve the energy conversion efficiency from the Tx source to the received DC energy/power for WPT and maximize the received power from the environment for WEH.

It should be pointed out that energy conversion efficiency is generally used to assess the performance at Rx for both WPT and WEH. Power transfer efficiency (PTE) is often used to assess the performance of a WPT system, and it is defined as the ratio of the RF power transmitted at the Tx and the received DC power at the Rx.

IV. Metamaterial and Metasurface based Non-Radiative WPT

In a typical WPT system, metamaterials, particularly in their 2D form as metasurfaces, have been proved to be extremely useful in many different applications [9], [32]-[36], especially in improving the PTE and increasing the power transfer distance. A useful review of metamaterial and metasurface-based WPT systems has been carried out based on the dimension (1D, 2D or 3D) and the configuration of the slabs [37]. A slab can be placed in the middle, front, back or side of the Tx-Rx structure. The performances of different configurations are summarized and compared using a figure of merit, which was defined as the PTE times the ratio of the transfer distance over the coil diameter.

In this paper, it is analysed how metamaterials and metasurfaces can manipulate electromagnetic waves for WPT and WEH. The latest progress on metasurface-based design techniques to enhance WPT performance will be reviewed. These design techniques will be divided into three categories based on how they change electromagnetic wave propagation: shielding/reflecting, focusing/concentrating, and guiding/directing. Typically a metasurface slab can be added behind the Rx or Tx to reflect electromagnetic waves, and enhance the coupling between the Tx and Rx. The slab can also be side placed to shield electromagnetic waves, to both improve PTE and reduce electromagnetic leakage or interference. A metasurface slab should be inserted between the Tx and Rx to focus electromagnetic waves. In a few other application scenarios where the location and position of an Rx are not fixed, metasurfaces can be reconfigured to direct electromagnetic waves. These methods can be combined in one design for some applications.

A. Metasurface WPT Systems Based on Shielding

In the simplest scenario, a WPT system consists of a Tx and an Rx of a planar structure. The magnetic fields of the Tx are symmetrical on both sides.

One very intuitive way to improve the WPT performance is to confine the magnetic fields to the region between the Tx and the Rx. The effectiveness of shielding for improving the performance of WPT was analyzed in [38]. It was shown by adding two ferrite slabs behind the Tx and Rx coils, not only the EM field leakage was reduced by 92%, but also the PTE was increased from 14.3% to 37.1%. It was further demonstrated that by adding a pair of metasurfaces between the Rx and Tx, the PTE can be improved to 52.4%.

While natural materials such as ferrite can be used for magnetic shielding purposes [39], they are usually lossy, bulky, and heavy. Resonant structures can be used instead for shielding to improve WPT efficiency and distance [40]-[42]. In [43], a metasurface with an effective permeability close to zero was placed behind the Tx and Rx of a near-field WPT system to reduce EM field leakage. Another metasurface with a negative effective permeability was placed between the Tx and Rx to improve PTE further, the concept of which will be discussed in the next subsection. The unit cell of the shielding metasurface was a coil of a square spiral pattern printed on the top of a slab. A lumped element capacitor was added between the two ends of the spiral coil to tune the operation frequency. Each unit had a length of 12 cm, which was 1/184 of the wavelength. The total shielding metasurface with 3 × 3 unit cells is shown in Fig. 4. At a transfer distance of 40 cm, the PTE was increased from 36% to 48%.

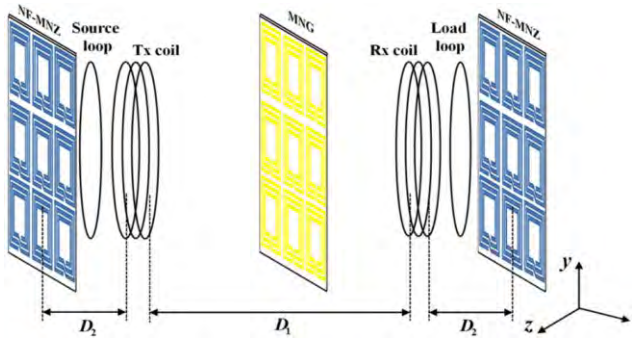

Fig. 4. A WPT system with a pair of metamaterial slabs for shielding and one metamaterial slab for improving efficiency [43].

The reflection metasurface can also be arranged in a non-planar way [40]. One design with reflection shielding elements is shown in Fig. 5. The Tx and the Rx were coaxially aligned as shown in Fig. 5 (a). One and two reflective elements were added as shown in Fig. 5 (b) and (c), respectively. Their separation was $\Delta z = \lambda/1000$. The distance between the Rx's and the main Tx's was $d = 0.1\lambda$ in all three cases. The operating frequency was 13.56 MHz. As demonstrated in [40], [42], by adding one or two elements, the PTE can be increased from 13% to 21%

and 26%, respectively. It is very interesting to note that in this design the added elements can be active ones as well. But the maximum achieved PTEs are very close to each other when the added elements are passive or active, in optimized conditions.

It should also be noted that the structures shown in Fig. 5 are not relaying systems for two reasons. One is that, in this setup, the Tx is the one closest to the Rx. The minimum distances between the Tx and Rx are the same in these three structures. The reflecting element(s) are on the other side of the Tx, and are further away from the Rx. Therefore the added elements do not relay power. The other reason is that the added elements do not resonate at the same frequency as the Tx and Rx. Their main function is to reflect electromagnetic waves and enhance the coupling between the Tx and Rx.

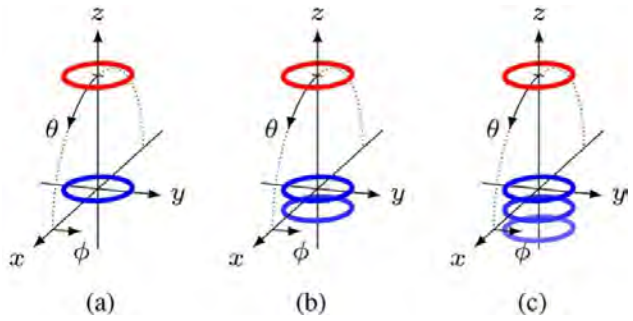

Fig. 5. The WPT setup with multiple Tx's shown in blue. The Rx is shown in red. (a) The coaxial Tx and the Rx, (b) one reflecting element was added beneath the Tx, (c) two reflecting elements were added beneath the Tx [40].

The idea of shielding using resonant structures has been used to address the health and safety concerns of WPT. The concept of resonant reactive shielding for WPT systems, especially for high-power applications, is shown in Fig. 6 [39], [44]. Using this method, a 12-turn resonant reactive shield and its automatic tuning system were applied for a 5-kW WPT system. The magnetic field at the observation point outside of the shielding coil was reduced from 11 T to 1.3 T. In this design, the Tx and Rx were resonant at 20 kHz.

There are other methods to provide shielding using metamaterials [45]-[47]. A comprehensive analysis and review of side-placed metamaterials in WPT systems were provided in [48]. It was demonstrated that side-placed metamaterial can also enhance the tolerance to the misalignment of coils for WPT.

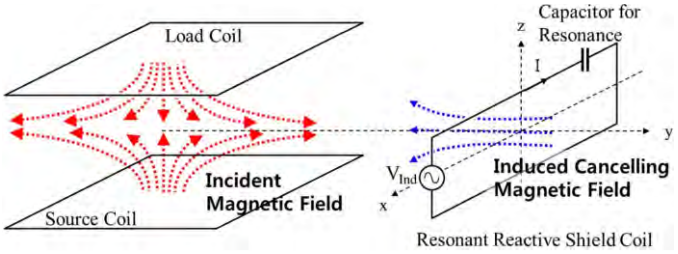

Fig. 6. Suppression of the magnetic field leakage at the side of an electric vehicle [44].

Metasurfaces can also be used to shield the fringing field of capacitive WPT systems, as shown in Fig. 7 [49]. This design is suitable for MHz range wireless charging systems with large air gaps. Experimental verification was carried out using two WPT systems operating at 13.56 MHz with an air gap of 12 cm: the capacitive meta-coupler-based system and the inductive one exhibit significantly smaller fringing field levels compared to the conventional one (just two parallel plates). The inductive one is slightly more effective for suppression, but the capacitive one can achieve slightly higher efficiency. The meta-couplers were implemented using 12-cm diameter circular plates and 22-cm outer-diameter copper rings placed concentrically with a 1-cm air gap between them. It was shown that by utilizing metasurface-based coupling plates [49], the fringing electric field could be reduced by 40% in magnitude.

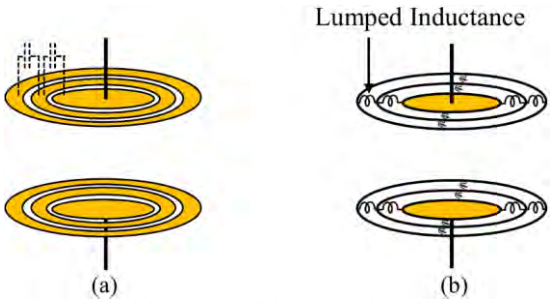

Fig. 7. Suppression of the fringing field. Physical implementation of a meta-coupler using (a) a capacitive metasurface and (b) an inductive metasurface [49].

B. Metasurface WPT Systems Bases on Focusing

By far, the most common way to enhance WPT performance is to focus/concentrate EM waves in the region between the Tx and the Rx. In the literature, there are a number of designs of metasurface-based WPT systems based on focusing [50]-[58]. The fundamental concept is shown in Fig. 8 [59]. A metasurface is inserted between a Tx and Rx to improve the performance of the WPT. The metasurface works as an effective superlens to manipulate the EM field in the region. The control of the effective magnetic permeability of the metasurface is vital for the WPT system. The theory of a near-field metamaterial superlens has been studied in [59]-[61]. A general analytical procedure to characterize a metasurface through an equivalent lumped-element circuit for resonant inductive WPT has been presented in [59]. It was shown in [60] that the PTE could be an order of magnitude greater than free-space cases with a properly designed metamaterial slab. It was also found that the volume of the metamaterial could be greatly compressed by employing magnetic permeability with a large anisotropy ratio. In [61], the Tx and Rx were approximated as point-dipoles to calculate the fields of the coils. Based on this approximation, closed-form and analytical expressions were obtained to explain why the PTE could be improved with a metasurface.

While it is possible to concentrate the EM field using beamforming techniques with an antenna array [62], the operation of a metasurface is quite different from that of an antenna array. The units on the metasurface are usually non-uniform resonating at slightly different frequencies to provide the metamaterial effect. As illustrated in Fig. 9, the area in the center could have a different effective permeability from the edges [63], [64]. Such a metasurface is sometimes called a hybrid metamaterial slab. The units in the center usually have an effective permeability close to zero, to ensure the magnetic field in the center area will straightly pass through the center units and reach the Rx. The hybrid slab has an effectively negative value of permeability on the edges, to re-redirect the

magnetic field to the Rx and hence improve the WPT performance. In practical designs, the permeability can be altered gradually, rather than sharply.

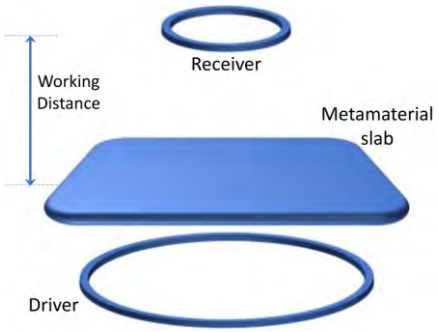

Fig. 8. Schematic of a WPT system consisting of a transmitter (driver) and a receiver coupled through a metamaterial slab, or a 2D metasurface [59].

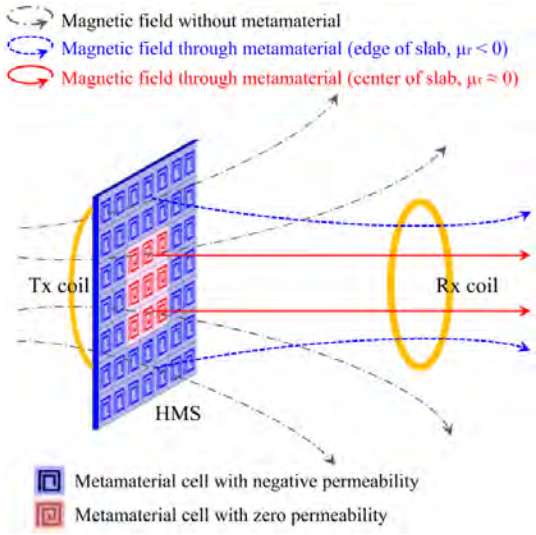

Fig. 9. The magnetic field distribution of a WPT system with a non-uniform metasurface between the Tx and Rx. The units in the center usually have an effective permeability close to zero, and an effectively negative value on the edges to confine the magnetic field between the Tx and the Rx [64].

In [65], a metamaterial cavity was designed for enhanced mid-range WPT performance. The cavity was realized by detuning a cell in the center to break the periodicity of the closely coupled metamaterial slabs, as shown in Fig. 10. The cavity helped the metamaterial slab to more effectively confine magneto-inductive waves in the region and provided enhanced power transmission. The leakage field to surrounding locations was reduced as well. With this method, the PTE was improved from 8.7% to 54.9%. In this design, the Rx is relatively small compared to the Tx and the slab.

The Huygens–Fresnel principle can be applied to develop metasurfaces as well [66]-[68]. The EM response of a Huygens's metasurface was investigated in [69]. It could provide beam shaping, steering, and focusing capabilities. In [66], a Huygens' surface was realized to implement both electric and magnetic polarization currents to generate prescribed wavefronts. It was embedded between the Tx and Rx in a near-field WPT system in [69]. A thin-layer and finite-size metasurface consisting of 64 elements was designed using bi-anisotropic Omega-type particles at the frequency of 100 MHz, as shown in Fig. 11. It was shown that the PTE was increased from 25% to 42% with the presence of the proposed metasurface.

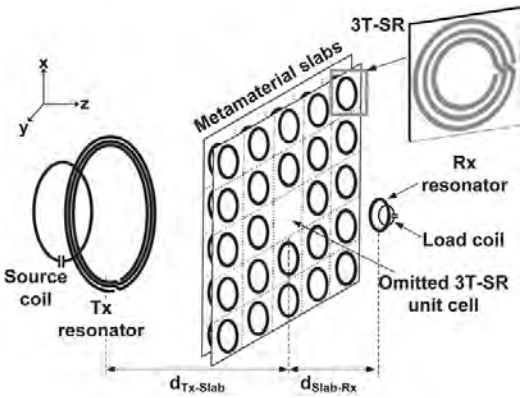

Fig. 10. Schematic of the WPT system with metamaterial slabs. The center cell was detuned to improve transmission efficiency [65].

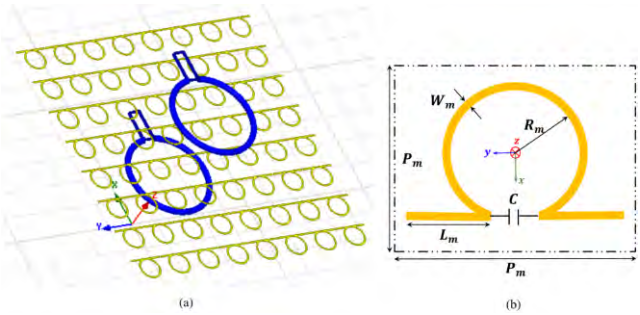

Fig. 11. (a) Configuration of the WPT system using a Huygens's surface and (b) sketch of the Omega-type particle forming the metasurface [69].

Dielectric resonators can be used to construct metamaterials too. A metamaterial-coupled high-efficiency WPT system was designed using cubic high-dielectric resonators [70]. The proposed WPT system consisted of two metamaterials separated by a distance and excited by two rectangular coils as shown in Fig. 12. One very useful feature of this design is that it was less sensitive to the misalignment of the Rx coil, compared with most inductive coupled WPT systems. The PTE due to misalignment of the Rx could be mitigated by rotating the dielectric resonators. High permittivity microwave ceramic materials samples were used to construct the metamaterial tubes for experimental verification. The cubes were surrounded by Teflon to make resonators. The WPT system achieved 52% efficiency at a distance of 0.2λ and more than 80% efficiency at shorter distances. It was found that dielectric resonator-based systems could outperform other WPT systems in terms of efficiency, range, size, and specific absorption rate.

Most WPT designs reported in the literature are based on magnetic/inductive coupling. With a high value of effective permittivity generated by metamaterial, a strong magnetic dipole behavior can be excited. The magnetic field will be extended further from the Tx. A strong magnetic coupling can be produced between the Tx and Rx, hence improving the PTE. Therefore a high permittivity or a zero/negative permeability would be beneficial for WPT. Metamaterials with a high permeability have been less reported. Another reason is that suitable natural high-permeability materials, such as ferrite and nanocrystalline materials, widely exist.

The performance of a WPT system can be improved by the high permittivity property of a metamaterial rather than its negative permittivity or permeability property. In [71], the unit cell of a metamaterial slab was realized by using circular SSR resonators. By increasing the length of the strips in a spiral manner, the real part of the relative effective permittivity could reach an extremely high value (> 800), as well as negative values at different frequencies. A WPT system making use of such a high permittivity property was demonstrated in [72], as shown in Fig. 13. Magnetic field distribution with or without the metamaterial slab was analysed in this paper. It was demonstrated that the magnetic coupling between the Tx and Rx can be significantly enhanced with the slab. Experimental results showed that the PTE could be improved from 52.2% to 60.8% at 472 MHz when using the material slab.

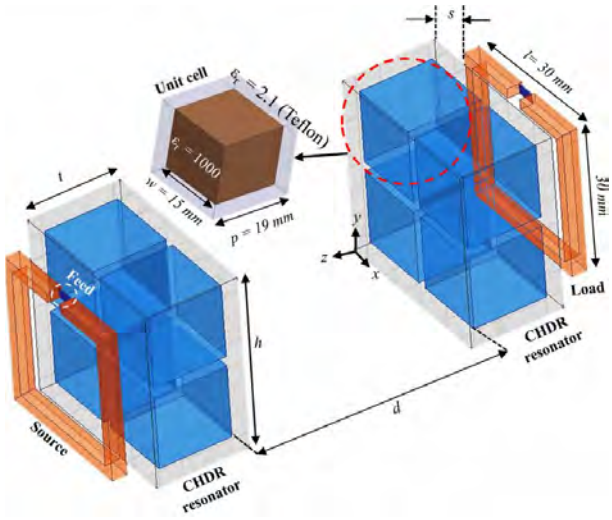

Fig. 12. A metasurface based WPT system using cubic high-dielectric resonators [70]

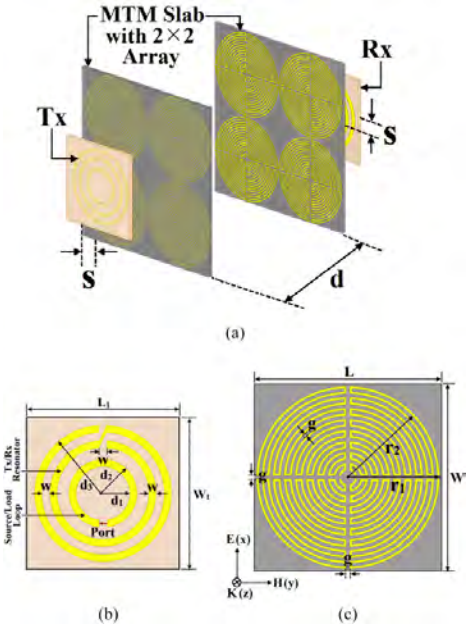

Fig. 13. (a) Schematic of a WPT using metamaterial slabs with high effective permittivity. (b) Top view of the Tx/Rx and (c) Schematic configuration of the unit cell of the metamaterial slab [72].

One very important application of metasurface-based WPT systems is for medical implantable and wearable devices [73]-[76]. A very compact metasurface potentially suitable for wearable and implantable applications is shown in Fig. 14 [73]. Each unit cell consisted of connected double-spiral coils on two sides of a slab. Due to the way the coils were connected, the slab could be very thin and compact. By adding a slab with a size of 6 cm × 6 cm and a thickness of 1 mm, the PTE was increased from 5% to 7% at a distance of 25 mm when the slab was added on the Tx side, and to 12% when another slab was added on the Rx side. The operating frequency was 6.06 MHz. It was observed that the metasurface was also able to reduce the electric field dramatically by about 90%. One important concern on the safety of WPT systems for implantable applications is the effect of electromagnetic fields on the human body. Specific absorption rate (SAR) is a commonly used measure of the rate at which energy is absorbed per unit mass by a human body when exposed to an RF electromagnetic field. SAR is proportional to the square of the magnitude of the electric field. Having a much reduced electric field made the design very suitable for wearable or implantable applications.

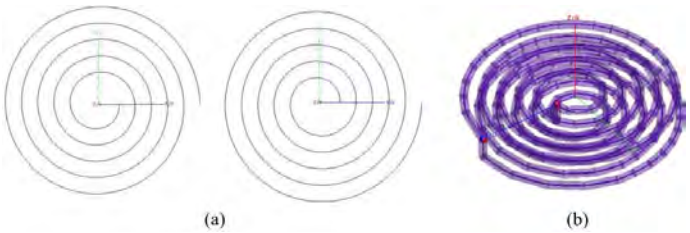

Fig. 14. The two spirals in a unit cell have different orientations of windings. (a) Top views of the two separated spirals that were used to construct a unit cell. (b) Picture of a complete unit cell [73].

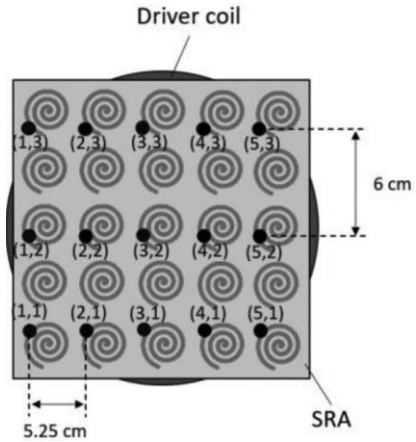

Fig. 15. A spiral resonator array is designed to both increase the power transfer efficiency and reduce the electric field exposure for near-field WPT [75].

A method to reduce the specific absorption rate associated with electric field for near-field WPT is to use a metasurface constructed by a spiral resonator array as shown in Fig. 15 [75]. By using an array on the Tx side only, it was possible to not only lower the electric field exposure but also enhance the efficiency level. With a 5 × 5 matrix of passive resonant spiral resonators, the PTE was improved from 5.5% to 32.9%, and the electric field was reduced by 60% in magnitude. Such a feature can be very useful for biomedical, implantable, wearable, and automotive applications.

A miniaturized implantable antenna was proposed for cardiac pacemaker applications in [76]. To improve the PTE, a metasurface was designed in a planar reverse spiral structure on both sides of a slab. The elements had a size of 10.5 mm × 10.5 mm × 1 mm operating at 430 MHz. The elements were grouped into a 2 × 2 array. The metasurface had a strong magnetic resonant behavior to improve the PTE of the WPT system. It should be pointed out that in this application, the metasurface was implemented on the Rx side only, as shown in Fig. 16. It was notable that, with the metasurface, the transmission coefficient was 11 dB higher at the resonant frequency than the case without the metasurface. The PTE improvement was very significant between 400 MHz and 450 MHz by adding the metasurface.

C. Metasurface WPT Systems Based on Guiding

The WPT systems discussed in Sections IV.A and IV.B usually have their Tx and Rx in fixed positions to achieve high PTE, normally aligned in a line or a coaxial manner. In real-world applications, the Tx and Rx may not be aligned in this way. In order to improve transmission efficiency, relay resonators can be used to improve PTE and transfer distance [77]. It was demonstrated in [78] that such relay resonators could be arranged in various domino forms as shown in Fig. 17. General analysis on WPT with non-coaxial axes was carried out in this work. Mathematical formulations were established to analyze resonator systems with various domino forms. WPT systems with circular structures and with more than one main power flow path were analyzed using a superposition method. Unlike traditional relay systems [79], it was demonstrated that optimization of the domino systems could be achieved under non-resonance frequencies, hence it could be regarded as a system with metamaterial characteristics. In [78], the structures with metamaterial characteristics were utilized to direct/guide EM waves, so as to transfer power in a non-coaxial direction or with more than one power flow path.

In addition to non-coaxial and multi-path applications, in many other cases, the Rx might be placed in non-fixed positions, or multiple devices might need to receive power simultaneously at different power levels. In these applications, the intensity and the shape of the field-localizing area should be dynamically controlled.

There are various techniques to implement high PTE with high flexibility and reliability without dynamic control [4], [80]. However, there can usually be only one Rx in such systems to maintain high PTE. It was demonstrated in [81] that by introducing defects, it was possible to dynamically control the propagation of magneto-inductive waves on a 2D metamaterial. A dynamic control mechanism was proposed for directing power or data transfer to a specific area on the metamaterial.

The concept of a hotspot or power-focused region using field-localizing WPT with an active metasurface to achieve multiple functionalities was introduced in [82]. Using this method, it was demonstrated that the location, shape, and intensity of the hotspot could be manipulated as desired. The power can be directed to intended devices while reducing leakage to other areas, as shown in Fig. 18. To dynamically reconfigure the hotspots and focusing areas, the metasurface elements were dynamically switched and tuned. The dynamic reconfigurability can overcome the limitations associated with passive metamaterials. Because the location, shape, and intensity of hotspots can be controlled, multiple devices can receive power at variable locations at different power levels with high PTE. It should be noted that such active metasurfaces are usually designed to shape and direct WPT dynamically. The absolute maximum power transfer efficiency of these systems would not necessarily be higher than a well-aligned passive WPT system. The main advantages of WPT systems using active metasurfaces are the improved flexibility, reliability, and safety, especially for WPT systems with multiple receivers.

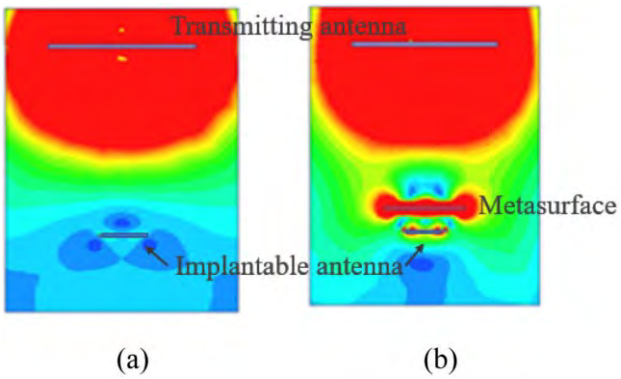

Fig. 16. Magnetic field distribution of the WPT system: (a) without the metasurface and (b) integrated with a metasurface on the Rx side [76].

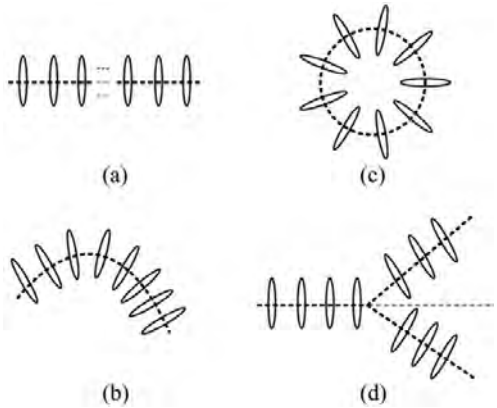

Fig. 17. Implementation of WPT systems using various domino forms of relay resonators [78].

Wire media, or arrays of parallel metal wires, have been applied for various applications. One property of wire media potentially useful for WPT is the efficient conversion of evanescent waves into waves propagating in the wire medium [83], [84]. In [85], a smart table was designed using a wire array as shown in Fig. 19. The wire array was used to enhance the coupling between two dielectric resonators placed in the near field of the surface. For a disk resonator with high permittivity operating in a magnetic dipole mode, the electric field is mostly concentrated inside. The magnetic field is high near the surface [85], [86]. When a wire medium is nearby, the resonator may be strongly coupled to the wired medium. The near magnetic field of the Tx resonator can be converted into propagating modes of the wire medium. The power can then be transferred

from one resonator to another along the wires. A smart table with multiple Rx's was proposed in [87]. A capacitive WPT platform using an active metasurface to support multiple Rx's was reported in [88].

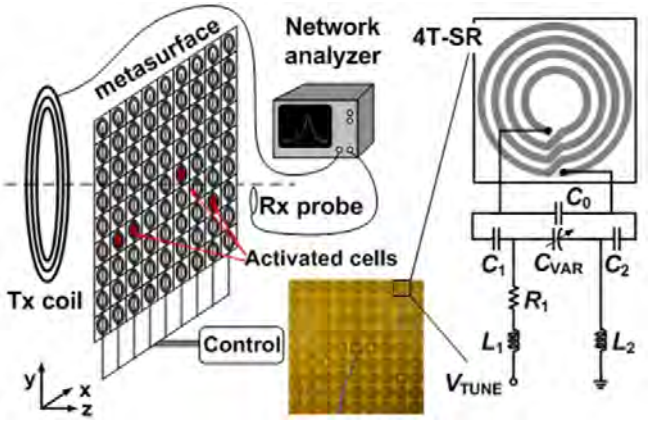

Fig. 18. Schematic and photo of an active metasurface. The unit cell has a tuning function [82].

It is possible to improve WPT performance by dynamically changing material parameters using tunable metamaterials. In [89], [90] liquid crystal and ferrite were investigated as tuning materials to construct metamaterials. Switches such as PIN diodes and tunable capacitors and inductors can also be used as variable elements to tune the characteristics of a metasurface. However, the computational complexity is the main challenge for these applications, especially when the number of unit cells is increased, the size of the Tx is getting large, or the expectation of freedom in terms of flexibility and reliability is high.

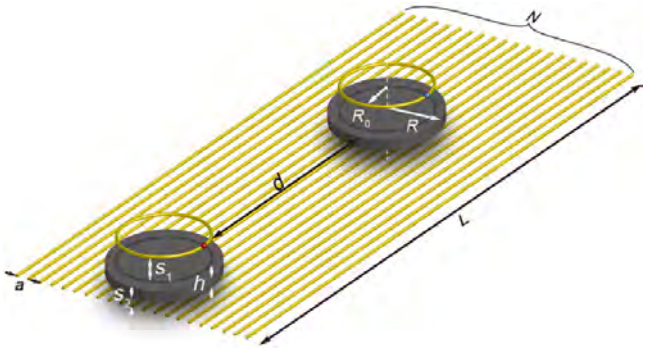

Fig. 19. Schematic diagram of a WPT system based on dielectric resonators above a wire medium [85].

In [91], a deep neural network-based design of tunable metamaterials for WPT was investigated. Using structures specifically designed for different tasks, the neural network could predict the frequency spectra and synthesize unit cells' design parameters for a given metasurface geometry. A generative model of the deep neural network was used in [92]-[94] to replace the conventional trial-and-error approaches for the design and configuration of metasurfaces. With sufficient data training, the data-driven method was also extended to create different WPT paths between the Tx and Rx and predict the frequency spectra of them. It was experimentally demonstrated that it was feasible to direct power to multiple devices using different paths as shown in Fig. 20. Peak efficiency of 56.8% was achieved. It is also of particular interest to note that different WPT paths can be generated with obstacles placed on the metasurface.

D. Discussion of Metasurface-Based Near-Field WPT

The performance of metasurface-based WPT systems using the shielding, focusing, and guiding techniques are summarized in Table I. It can be seen that the PTE of WPT has been greatly improved in all cases. Especially for the focusing/concentrating techniques, the improvement can be drastic as shown in [65], [75]. In these two cases, the PTE was increased by more than six-fold from 8.7% to 54.9% and from 5.5% to 32.9%, respectively.

With the shielding/reflecting technique, metasurfaces can improve the PTE at a moderate level. But they can be used to suppress either the electrical field or magnetic field for EM compatibility purposes, by reducing field leakage or guiding power to desired locations. The guiding/directing technique is usually associated with the dynamic control of metasurface elements. This technique is particularly suitable for the scenario where the Rx is not at a fixed position or needs to receive power at a variable level. In these applications, a metasurface is an enabler. The PTE would be otherwise extremely low without a metasurface and the dynamic control of its elements.

It should also be noted these techniques can be combined. For example, both shielding and focusing metasurfaces were used in [43]. A focusing/concentrating metasurface can also reduce the electric or magnetic field as shown [73], [75]. Fundamentally, a metasurface is a media that can be used to improve the performance of WPT by manipulating the EM field in the desired manner.

V. Metamaterial and Metasurface-Based Radiative WPT and WEH

Non-radiative WPT has a limited range and is suitable for short to medium-distance applications. For longer distances, radiative WPT becomes a feasible solution [95] although laser WPT is another approach but not discussed here. The radiative WPT can work from the radiative near-field region (the Fresnel region) to the far-field of the transmit antenna. For radiative applications, metamaterials and metasurfaces are more commonly used to improve the performance of WPT. Here we will first discuss metamaterial and metasurface-based WPT technologies and then review the applications of metamaterial and metasurfaces on WEH.

A. Metamaterial and Metasurface-Based Radiative WPT

For radiative WPT, two types of metamaterials and metasurfaces are commonly used: beamforming and reflective ones.

1) Beamforming metamaterials and metasurfaces for WPT

The boundary between the far-field and the Fresnel region is usually taken to be the distance of $2D^2/\lambda$, D being the maximum dimension of the transmitting aperture. This distance is required in order that there be no greater phase differences than $\pi/8$ radians at a point in the space from any point in the aperture. In the far-field region, the phase difference can be ignored. So by feeding each unit of the antenna array with equal

Table I Performance comparison of metasurface-based non-radiative WPT systems using different techniques to control EM fields (Dia denotes diameter).

Ref. (year)	Freq (MHz)	Metasurface Size (cm)	Tx/Rx Size (cm)	Tx/Rx Gap (cm)	Type of Operation	Efficiency Improvement (%)	Notes
[38] (2016)	6.78	80×80	40×40/ 40×40	50	Shielding Shield/focusing	14.3% to 37.1% 14.3% to 52.4%	Magnetic field shielding
[43] (2019)	13.56	36×36	Dia 20/ Dia 20	40	Shield/focusing	36% to 48%	Magnetic field shielding
[49] (2020)	13.56	Dia 22	Dia 22/ Dia 22	12	Shielding	NA	Electric field reduction
[75] (2020)	13.56	18×18	Dia 18/ Dia 18	16	Focusing	5.5% to 32.9%	Electric field reduction
[64] (2018)	6.78	26×26	15×15	15	Focusing	34.5% to 41.7%	Non-uniform
[65] (2016)	6.5	>50×50	Dia >50/ Dia 40	55	Focusing	8.7% to 54.9%	Non-uniform
[69] (2020)	100	33×33	Dia 32/ Dia 32	40	Focusing	25% to 42%	Units connected
[70] (2018)	560 1700	3.6×3.6 5.3×5.3	3×3/3×3 5×5/5×5	10 3.6	Focusing Focusing	58.5% 52%	Dielectric resonator
[72] (2019)	472.6	8×8	4×4/ 4×4	36	Focusing	To 60.8%	High permittivity
[73] (2020)	6.06	6×6	Dia 4.2/ Dia 4.2	2.5	Focusing	5% to 12%	Low specific absorption rate
[82] (2019)	14.1	>51×51	Dia 25/ Dia 3	20	Guiding	7.8% to 50.4%	Active metasurface
[91] (2020)	14	>54×54	Dia 6/ Dia 6	3	Guiding	Peak 56.8%	Smart table

amplitude and in-phase, a far-field high-gain beam can be realized. While in the Fresnel region, the existence of the phase difference allows us to realize the regulation of near-field beams, such as near-field focusing (NFF) beams [96], [97], non-diffraction beams (like Bessel beam) [98], etc.

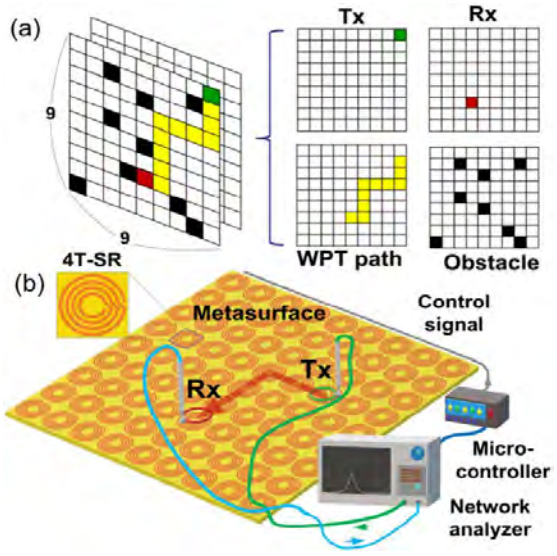

Fig. 20 (a) Schematic of the grid map of a metasurface designed based on a deep-neural network. (b) Experimental setup to collect training data [91].

Among these beam forms, NFF, as a unique feature of antennas operating in the near-field region, has attracted the attention of researchers. When the transmitting aperture qualifies a concave spherical phase front, the EM wavefront will form a convergent focus in the near field region. Wireless power will achieve a denser electric field distribution characteristic on the target aperture, thereby greatly improving the transmission efficiency. NFF has been implemented through a variety of antenna forms, such as parabolic reflector [99], dielectric lens antennas [100], microstrip phased array [101]-[102], [103], [104], planar FZP (Fresnel zone plate) lens [105], [106] and leaky-wave antennas [107], [108], etc. However, the drawbacks of high processing cost, huge volume, complex feeding network, and limited efficiency restrict the utilization of NFF in efficient WPT. An implementation method that can balance cost and efficiency with simple structures is needed. For far-field radiative WPT, antenna arrays have been widely adopted for beaming forming [109]-[113]. Capabilities of such designs are often hindered by the high cost and complexity of electronically scanned antenna systems, relying predominantly on active components. Metamaterials and metasurfaces possess the ability to flexibly adjust the amplitude, phase, polarization, and other characteristics of incident EM waves, suggesting a simple but effective alternative solution to this issue. They can provide nearly equivalent performance with passive components, avoiding the need of phase shifters and amplifiers in conventional systems. In recent years, scholars have introduced the combination of metasurfaces and NFF for RF [114], mid-near infrared [115], and even underwater ultrasound [116] applications. A fan-shaped beam was generated by using a metasurface in [117]. The wavefront was shaped by using a genetic algorithm to obtain the optimal phase and amplitude distributions, with the ability to form arbitrary beam shapes. A metasurface using C-shaped elements was reported in [118]. The metasurface could generate and control multiple beams simultaneously. The intensities of multiple beams can be separately modulated as desired benefitting from the independent controls of phase and amplitude profiles. A waveguide-fed metasurface antenna architecture that enables electronic beamsteering from a lightweight circuit board with varactor tuned elements was

reported in [119]. It was experimentally demonstrated that Nyquist metasurface antennas can realize high-performance beamsteering without phase shifters, making them a compelling technology for the design of future beamforming hardware.

2) Reflective metamaterials and metasurfaces for WPT

In 2019, [120] proposed a reflective metasurface with multi-focus characteristics, whose schematic diagram is shown in Fig. 21. A general synthesis procedure was outlined to design reflective metasurfaces with multi-feed and multi-focus, connecting seamlessly with the multiple-input multiple-output (MIMO) WPT requirements of wireless sensor network (WSN) applications. Specifically, the metasurface element can present different reflection phase shifts at 5.8 GHz by adjusting the dimensions of the designed tri-dipole structure. According to the required phase compensation distribution, the proposed 20×20 metasurface array could realize several NFF beams, forming efficient spatial synthesis and diversity of wireless power. A maximum NFF transfer efficiency of 70% was achieved at a distance of 1 m with a metasurface of the size of 500 mm × 500 mm, and the relative bandwidth with 50% efficiency was about 16%.

On this basis, [121] further realized the multi-focus unequal power distribution characteristics through the metasurface elements with dual-polarization independent regulation characteristics for the requirement of MIMO WPT applications. By adjusting the polarization angle of the feeding horn, the designed 'cross-dipole' structure could perform orthogonal polarization decomposition of the incoming wave, thereby achieving two beams with unequal power distribution, greatly improving the flexibility and practicability of MIMO WPT. The measured near-field scanning results are shown in Fig. 22. The cases of single focus, dual-focus, and single focus with dual-polarization could realize a peak efficiency of 71.6%, 68.3%, and 65.9%, respectively.

3) Other radiative WPT techniques

In addition to beamforming and reflection, flexible regulation of radiative WPT is also a noteworthy application requirement. [122] proposed a reconfigurable holographic metasurface operating at 20 GHz with PIN diodes loading to realize dynamic WPT. The WPT system characteristics could be reconfigured. It can focus at any desired position in the near-field through controlling the bias applied to the diodes. Some other numerical designs of reconfigurable metasurfaces have been proposed in recent years. However, they also faced the challenges of system complexity and efficiency. In 2019, a polymer transmit metasurface [123] was proposed to realize WPT, adopting 3D printing technology to replace the conventional PCB process for reducing processing costs.

Typical unit cells of metasurfaces that have been developed for radiative WPT, as discussed above in this subsection, are summarized in the first row of Fig. 23.

B. Metamaterial and Metasurface Based WEH

WEH is another hot topic related to WPT. As discussed in Section III, these two are similar, but there are clear differences. Table II compares RF/microwave WPT and WEH in detail.

Metasurfaces have shown the characteristics of miniaturization due to their sub-wavelength periodicity. Through the close periodic arrangement, metasurfaces can achieve a strong resonance effect with near-unity harvesting efficiency (defined as the ratio of the time-average power received by the metasurface over the time-average power incident on the entire metasurface.). The requirements of WEH such as bandwidth, beamwidth, and polarization-insensitivity can be improved by the use of metamaterials and metasurfaces. A comprehensive survey on recent advances in metamaterial/metasurface-based WEH systems has been carried out in [124]. An overview of WEH sources and various designs of rectenna at different operation frequencies are also provided in this work.

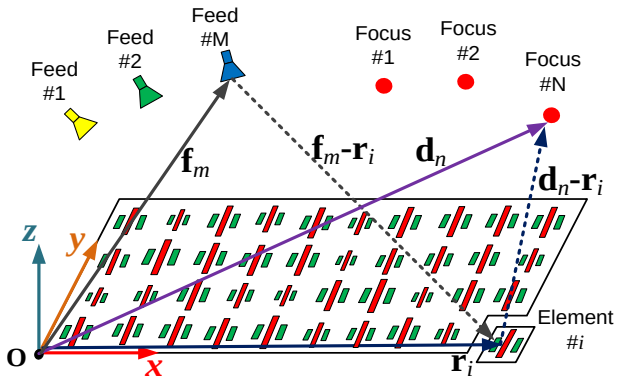

Fig. 21 Geometry of a reflective metasurface for the multi-feed and multi-focus WPT system [120].

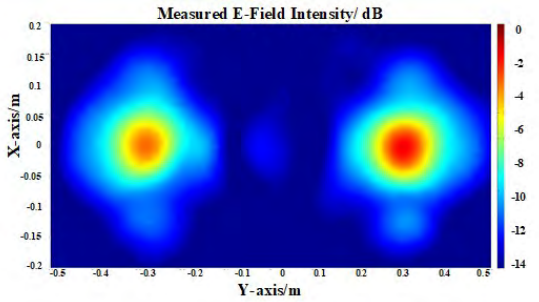

Fig. 22 The normalized near-field scanning measurement results of E-field intensity for single-feed and dual-focus reflective metasurface: unequal power distribution in x-direction polarization excitation [121].

1) Wideband WEH

An excellent EM absorber was realized through metasurface design in 2008 [125]. But for WEH, the goal is to maximize the capture of RF energy, rather than dissipating energy into the structure like the absorber. The absorber could be considered as the rectenna load for storage or applications. In 2012, [126] presented that metamaterial particles could act as energy harvesters when a resistive load was inserted within the particles' gap. An SRR operating at 5.8 GHz was proposed as a unit cell to form a 9×9 array to replace conventional antennas to realize RF energy harvesting.

However, the harvesting efficiency of the original design was less than 80% due to the without-ground-plane structure and suffered from incident-angle-sensitivity as well as narrow bandwidth due to the strong resonance characteristic [127-128]. In 2015, an improved design was proposed by using a planar array composed of subwavelength electric-inductive-capacitive resonators [129]. The significant difference from the SRR is

Table II Detailed comparison of RF/microwave WPT and WEH

	WPT	WEH
Main Requirement	High Energy Transmission and Conversion Efficiency	
Application Scenarios	Mid to High Power Devices	Low Power Sensors
Transmitting-Receiving	Point-to-Point	Space-to-Point
Operating Frequency	Dedicated Narrowband	Communication Bands, ISM Bands, etc. Wideband/Multi-band
Antenna Pattern	High Gain/Directivity	Wide Incident Angle (Omni-Directivity)
Polarization Requirement	Alignment	Polarization Insensitive
Key Issues	Antenna Wavefront Regulation	Rectenna Impedance Matching Rectifying
Introducing Metasurface for	Wavefront Regulation (such as Near-Field Focusing)	Replacing Antennas to Harvest Wireless Energy
Required Characteristics of Metasurface	Amplitude/Phase Regulation Characteristics of Metasurface Units	Tight Coupling Effect Multimode Resonance Effect of Metasurface Arrays
Future Directions with Metasurface	Adaptive, Programmable, Intelligent Regulation Simultaneous Wireless Information and Power Transfer	Rectifying Metasurface Hybrid Energy Harvesting for Energy Autonomous of WSN

that the electric-inductive-capacitive resonator has additional vias connecting the top layer and the ground plane. An up to 97% harvesting efficiency was achieved at 3 GHz under optimized conditions, suggesting that near unity RF harvesting could be achieved by using metasurfaces.

Since then, a large number of WEH metasurface unit cells with more abundant characteristics have been proposed relying on the two resonators. In 2015, [130] proposed a complementary SRR structure for efficiency improvement and bandwidth enhancement. A wideband ground-backed complementary split-ring resonator array [131] inspired by chaotic bow-tie cavities was also introduced with a half-power bandwidth three times higher than the previous work. [132] introduced a wideband metasurface array composed of square ring resonators with a half-power bandwidth of 110% (6.2 – 21.4 GHz). However, too many ports in the resonator made it not suitable for actual WEH applications.

2) Multi-band WEH

Designing metasurface unit cells with a multi-mode resonance effect is conducive to realize multi-band WEH. By arranging four SRRs rotational symmetry about the centre, the proposed design in [133] achieved a harvesting efficiency of 30%, 90%, and 74% at 1.75 GHz, 3.8 GHz, and 5.4 GHz in simulation, respectively. In 2017, [134] proposed a tri-band butterfly closed-ring resonator, covering the GSM (0.9 GHz), LTE (2.7 GHz), and WiFi (5.7 GHz) bands with wide-angle and polarization-insensitive characteristics. Two years later, [135], [136] extended the number of simultaneous operating bands to four by adding resonance at 2.6 GHz.

3) Wide-beamwidth and polarization-insensitive WEH

Sub-wavelength metasurface unit cells generally possess the structural characteristics of compact, miniaturized, and rotationally symmetric, demonstrating the advantages of insensitivity of polarization and incident angles. [137] proposed a circular SRR metasurface array to realize selective polarizations. The harvesting efficiency exceeded 60% at an incident angle up to 75°. To improve practicality, a compact single-band metasurface with a simple structure was introduced to acquire the wide-angle and polarization-insensitive characteristics and to reduce the number of ports in each unit cell [138], [139]. In 2020, a polarization-insensitive metasurface with up to a 75° incident angle was proposed in [140].

4) Effectiveness analysis and recent development

Regarding the effectiveness of metasurface-based EM energy harvester, a long-term discussion was how to compare the metasurface with antenna arrays in terms of size and efficiency. To address this, a comparative study between a metasurface using a ground-backed CSRR (G-CSRR) array and a patch antenna array has been presented in [141]. In this work, an 11×11 array of G-CSRR resonators and a 5 × 5 patch antenna array were designed at 5.55 GHz. The harvesting efficiency was observed to be 83% at 5.5 GHz for the G-CSRR cell and 60% for the patch antenna array. Due to the strong resonance and coupling between the metasurface unit cells, the G-CSRR array showed a wider half-power beamwidth (HPBW) than that of the patch antenna array at an oblique incident angle of H-plane and E-plane excitations. Therefore, it has been evident that the metasurface-based EM harvester could have a smaller size, a wider beamwidth, and higher aperture efficiency. But the challenge here could be the bandwidth issue [128], [131].

Recently, more novel features and multi-disciplinary integration technology have been introduced into the design of WEH metasurfaces. The proposal of a coded pixelated metasurface design could make the metasurface design fully automated [142]. The adoption of 2D-isotropic flexible materials for a metasurface could enhance the conformal capabilities of ambient harvesters [143]. Some work also focused on how to reduce the implementation cost of WEH metasurfaces [144].

A summary of important research progress in this field (in chronological order) is summarized and compared in Table III.

C. Rectifying Metasurface

The work discussed above in this section focused on RF energy capturing. The energy must be rectified for a complete energy harvester. Thus, inspired by the concept of ‘rectenna’, more and more research has begun to introduce metamaterials or metasurface into the rectenna design, to construct metamaterial-based rectennas.

Table III Comparison of performances among different WEH metasurfaces.

References (year)	Frequency (GHz)	metasurface Structure	Periodicity Metasurface Size	Maximum Harvesting Efficiency	Remarks
[126] 2012	5.8	SRR	0.18 λ_0 9×9	76%	first introducing metasurface to WEH
[129] 2015	3	ELC resonator	0.08 λ_0 13×13	97%	near unity efficiency
[130] 2015	5.55	Complementary SRR	0.34 λ_0 11×11	92%	efficiency & bandwidth enhancement than patch antenna
[133] 2016	1.75, 3.8, 5.4	Modified SRR	0.19 λ_0 7×7	30% at 1.75 GHz 90% at 3.8 GHz 74% at 5.4 GHz	triple-band polarization-insensitive
[137] 2016	2.47	Circular SRR	0.18 λ_0 15×15	97.2%	polarization selected wide-angle
[132] 2017	6.2–21.4	Square ring resonator	0.44 λ_0 5×5	96%	wideband polarization-insensitive
[134] 2017	0.9, 2.6, 5.7	Multi-mode closed-ring resonator	0.08 λ_0 7×7	90% at 0.9 GHz 83% at 2.6 GHz 81% at 5.7 GHz	tri-band miniaturized wide-angle polarization-insensitive
[141] 2018	2.45, 6	a ring resonator and a symmetric ELC resonator	0.09 λ_0 9×9	90%	pixelated metasurface algorithm optimization dual-band multi-Polarization
[128] 2018	2.45	mirrored SRR and hollow cylinders	0.16 λ_0 10×10	97.3%	wideband Wide-angle
[143] 2019	5.33	modified complementary SRR	0.13 λ_0 11×11	86%	flexible ultra-thin
[135] 2019	0.9, 1.8, 2.6, 5.8	4 nested SRR	43 mm 4×6	85.7% at 0.9 GHz 82.0% at 1.8 GHz 80.4% at 2.6 GHz 69.8% at 5.8 GHz	quad-band
[140] 2020	5.8	centrally symmetrical circular sectors surrounded by metal vias	0.29 λ_0 5×5	91%	frequency stability wide-angle polarization-insensitive
[145] 2020	2	circular loop with embedded dipole	0.13 λ_0 8×8	98%	dual-polarization no vias

For these rectennas, metamaterials were used as either parasitic elements or loading components to enhance the RF-DC conversion efficiency (defined as the ratio of the DC output power on a resistive load over the time-average power received by the metasurface) and reduce the rectenna size, rather than designing the complete metasurface plates as introduced in previous sections.

1) Conversion efficiency enhancement

In 2013, [146] introduced a 5×1 linear SRR array operating at 900 MHz with a rectification function. Its maximum RF-DC conversion efficiency was 36% (with an input power P_{in} of 24 dBm). Some metamaterial-based rectennas based on composite left/right-handed transmission lines or frequency selective surfaces have been proposed in recent years [147]-[150] to achieve miniaturization, multi-band, and better impedance matching.

Quite a few studies have tried to connect the designed rectifying circuits with WEH metasurface arrays to establish a complete RF-DC WEH link [151]-[153]. However, additional impedance matchings for multi-loads and a large-scale combining network would introduce more loss. Moreover, the existence of connectors often makes the overall structure poorly conformal. An effective solution is the coplanar integration of the metasurface and rectifying diodes to enhance the overall performance of the metasurface harvester, namely rectifying metasurface (also called metasurface rectenna or rectifying surface in some work).

The early rectifying surface had the defect of insufficient efficiency. A metamaterial rectifying surface [154] improved the total harvesting efficiency (defined as the ratio of the DC output power on a resistive load over the time-average power incident on the entire metasurface) to 66.9% at 2.45GHz under an incident power density of 5 mW/cm^2. The price to pay was that the structure was more complex and the matching network was retained.

More recently, [155] and [156] have proposed a variety of rectifying surfaces with different resonator structures, including tightly coupled antenna units, dipole units, and frequency selective surface units, etc. The total harvesting efficiency achieved was 40% and 61% respectively. A few typical rectifying surfaces with dedicated matching networks are summarized in the second row of Fig. 23.

The early concept of the rectifying surface for harvesting RF power with arbitrary polarization without a matching network was proposed in 2014 [157]. A harvesting efficiency of 25%

could be achieved by a 3 × 3 array at an RF P_{in} of −6 dBm. [158] introduced a coplanar rectifying surface including an I-shaped metasurface embedded with rectifying diode for space solar power satellite applications, achieving a harvesting efficiency of 28% at 0 dBm. A calculated harvesting efficiency of 50% at 0 dBm at 6.75 GHz was achieved in 2017 [159], based on a cut-wire metasurface with integrated diodes.

Further to [155], [156], on the basis of removing the matching network, in [160]-[162], the total harvesting efficiency was gradually increased up to 76% at 15 dBm. An 8 ×8 metasurface rectenna improved the harvesting efficiency to over 80% at 1.9 GHz with an RF input power of -5 dBm. However, the rectifying function was just realized on a 2×2 supercell, not the complete metasurface array [163].

In 2021, Li *et al.* [164] presented a dual-band, wide-angle, and polarization-insensitive rectifying metasurface with a miniaturized size, achieving a harvesting efficiency of 79% and 69% at 2.4 GHz and 5.8 GHz, respectively. Through a proper combination of the metasurface unit cells and diodes, the metasurface array could be integrated completely without the power combining network and the impedance matching network. A few typical rectifying surfaces with dedicated matching networks are summarized in the third row of Fig. 23.

Compared to a feeding network-assisted metasurface array, coplanar and double-sided rectifying metasurface could have a simpler configuration to avoid transmission lines used in the tiny space among those electrically small unit cells, thereby reducing the complexity of the feeding network and rectifier configurations. However, on the other hand, the simplified configuration of the rectifying metasurface also brings significant challenges in rectifier matching and optimization, especially, the unit cells are expertly designed to provide direct matching to the nonlinear impedance curve of the diode as a function of operating conditions. Therefore, multi-band and wideband rectifying metasurfaces remain a challenging topic and will need further efforts in future research to resolve issues related to the metasurface and rectifier integration [165], [166].

The rectifying metasurface generally integrates diodes on each unit cell or between the unit cells, and the positive and negative potential of the unit cell is determined by the metallization of the unit cell at both ends of the diode, so a DC output with positive and negative potential can be regarded as an independent power source. The DC output of each independent power source on the rectifying metasurface forms a DC synthesis network according to the series-parallel design, to combine the output DC power.

In the rectifying metasurface designs, an independent DC output is generally obtained by integrating diodes and determining the positive and negative potentials with 1 to 2 unit cells. The number of the used diodes mainly depends on the number of unit cells of the metasurface and the arrangement of the diodes.

The performance comparison of the state-of-the-art rectifying surfaces is provided in Table IV. It can be seen that in general the harvesting efficiency has been significantly increased over the years.

2) Circuit size reduction

Several metamaterial-assisted electrically small rectennas have recently emerged for IoT and wearable electronics [67], [68], [148], [149], [167]-[169]. In [148], metamaterial-inspired near-field resonant parasitic antennas were designed to directly match the input impedance of the rectifying circuit which decreased the overall size of the rectenna (ka ~ 0.611, where k is the free space wave number and a is the radius of the sphere that circumscribes the antenna). The rectenna size could be significantly reduced by having the near-field parasitic elements as shown in the bottom row of Fig. 23 whilst the experimental harvesting efficiency of this work was over 75% at 0 dBm power at the GPS L1 band (1.57 GHz). The work in [167] also showed an electrically small rectenna using such near-field resonant parasitics, with only 2.3 × 3 cm^2 size at 1.57 GHz and over 70% harvesting efficiency.

In [149], a compact composite right/left-handed-based dual-band rectenna was reported for 2.5 GHz and 3.6 GHz bands, as shown in the bottom row of Fig. 23. Having used the composite right/left-handed loaded structure, the size of the rectenna was reduced down to $0.3\lambda_0 \times 0.2\lambda_0 \times 0.0005\lambda_0$ where λ_0 is the wavelength at 2.5 GHz. The measured conversion efficiency of this compact rectenna was higher than 59% at 2.5 GHz and 41% at 3.6 GHz, for an input power of 2 dBm.

A Huygens dipole antenna is a type of metamaterial-inspired electrically small antenna which has a very compact size and relatively high gain. In [68], a Huygens rectenna was reported with two metamaterial-inspired near-field resonant parasitic elements, namely an Egyptian axe dipole and a capacitively-loaded loop, as depicted in the bottom row of Fig. 23. The prototype has achieved a gain of 4.6 dBi and a half-power beamwidth greater than 130°. The entire rectenna was electrically small with ka = 0.98 and tested 88% RF-to-DC conversion efficiency.

Motivated by the advantages brought by the Huygens dipole, a circularly polarized Huygens dipole rectenna was reported using a modified driven loop as a metamaterial loading and near-field resonant parasitic [168], [169]. The design example was an electrically small (ka < 0.77) and low-profile (0.04 λ_0) rectenna design at 915 MHz with CP feature and a relatively high RF-DC conversion efficiency of 89%, as shown in the bottom row of Fig. 23 [169].

These designs have shown the possibility of using ultra-compact rectennas for WPT and WEH applications, while the antenna characteristics in terms of gain, bandwidth, and efficiency could be significantly improved by these structures. By having a very compact size as a wireless energy reception node, these designs will be effectively adapted by IoT and communication devices requiring a small circuit footprint, such as implants, wearables, RFID, and backscattering tags. The research context and significant progress of metasurfaces applied to WEH are summarized in Fig. 23.

At present, metasurfaces are moving toward miniaturized, self-adaptive, programmable, and intelligent [170]-[174]. One very promising method for designing multi-band and wideband rectifying metasurface is to use the theory of characteristic mode analysis (CMA). The theory was established in 1970's [175][176] but re-visited in recent years for antenna design [177]. The bandwidth of an MTS based antenna can be broadened by exciting multiple modes on the MTS layer. The modes can be identified by CMA [178]. The design of a

Table IV Performance comparison of the state-of-the-art rectifying surfaces (including some metamaterial-based rectennas).

Ref. (year)	Freq (GHz)	Periodicity (mm) Num. of layers	Polarization Mode	Use of Matching Network	Type of Diode	Maximum Harvesting Efficiency	Structural Complexity
[157] (2014)	1	35×35 (single layer)	polarization-insensitive	No	HSMS-282C	25% at -6 dBm	simple
[158] (2014)	2.18	30×30×3.7 (dual layer)	linear	Yes	HSMS-2828	27.7% at 0 dBm	complex
[154] (2016)	2.45	20×20×4 (dual layer)	linear	Yes	HSMS-282B	66.9% at 5 mW/cm^2 (input power density)	complex
[155] (2017)	3	15×15×1.54 (dual layer)	linear	Yes	HSMS-2860	40% at 12 dBm	complex
[160] (2018)	2.84	50×50×3.175 (single layer)	linear	No	HSMS-2860	60% at 18.75 dBm	medium
[161] (2018)	3.4	18.7× 38.4×6.35 (single layer)	linear	No	HSMS-2860	76% at 14.3 dBm	simple
[162] (2019)	3	20×20×4 (dual layer)	polarization-insensitive	No	HSMS-2860	74% at 16 dBm	medium
[179] (2020)	2.45	24×24×4.3 (dual layer)	linear	Yes	SMS-7630	76.8% at 0.4 dBm	medium
[163] (2020)	1.9	25×25×18 (dual layer)	linear	No	SMS-7621	81% at -5 dBm	medium
[164] (2021)	2.4 5.8	16×16×1.27 (single layer)	polarization - insensitive	No	SMS-7630 (0 dBm) HSMS-2860 (10 dBm)	66% (2.4 GHz) at 0 dBm 55% (5.8 GHz) at 0 dBm 79% (2.4 GHz) at 10 dBm 69% (5.8 GHz) at 10 dBm	simple

broadband antenna using a nonresonant-cell metasurface with the aid of CMA was reported in [180]. A dual-polarized dual-layer metasurface lens based on split dipole unit cells has been presented in [181]. Also, the intelligent metasurfaces provide a brand new idea for the application of WEH, that is, making dynamic and instant optimized energy harvesting possible. There are still various ambient energy sources that can be harvested, such as solar, kinetic, thermal, etc. The hybrid energy harvesting [182], [183] based on multi-field integration of metasurfaces will also be an area worthy of attention.

VI. Discussion and Future Development

Usually, a metamaterial is any material engineered to have properties that are not found in natural materials. It is made from assemblies of multiple elements arranged in repeating patterns. Its elements should be much smaller than the wavelengths at the operating frequency. By engineering the arrangement of these sub-wavelength elements, the effective permittivity or permeability of the metamaterial can be tuned to positive, near-zero, or negative values.

Most WPT systems work in the MHz range. The size of elements is usually well below the corresponding wavelengths and only a limited number of elements are needed. Their effective permittivity or permeability could not be accurately extracted. If too many elements are used, the total size could be greater than the wavelength, but it would be too large for the desired application. Also, in most designs the elements are non-uniform and the elements are not strictly repeating themselves.

For WPT, WEH, and most other microwave applications, metamaterials are designed to manipulate electromagnetic waves by reflecting, absorbing, enhancing, or bending waves. The extraction of the effective permittivity or permeability is usually not necessary. They are able to manipulate and control electromagnetic waves to improve the performance of WPT and WEH, in a way that cannot be achieved by conventional materials. Especially for intelligent metasurfaces which are also reviewed in this paper, the elements are self-adaptive, programmable, and intelligent. The effective permittivity or permeability could only be extracted locally and dynamically.

In previous sections, metamaterials and metasurfaces based non-radiative and radiative WPT and WEH are reviewed systematically. Undoubtedly, over the years, the development of metamaterials and metasurfaces have made WPT and WEH one step further for practical real-world applications. In general, the following three aspects should be considered in the design of metamaterials and metasurfaces for WPT and WEH systems.

The first design consideration is the size reduction of the metamaterials and metasurfaces. In most designs as summarized in Table I, the size of the metasurface slab is larger than, or at least comparable to, the size of the Tx and Rx. This can be a concern in many cases. The slab is supposed to be an auxiliary part that is added to improve the power transmission, but it is actually bigger than the Tx itself. Wherever possible, the size of the slabs should ideally be much smaller than the Tx and/or the Rx. Also, for an electromagnetic field focusing metasurface, which is most widely used, the slab is usually inserted between the Tx and Rx. The distance between the Tx (or Rx) and the slab would be much shorter than the gap between the Tx and Rx. Therefore, the size reduction should be considered in the development of metamaterials for WPT and WEH. One potential solution is to combine the metasurface with the Tx or the Rx. In particular, metasurface-based antennas have been widely reported in recent years [178]-[181]. With this technique, the metasurface is an integral part of the Tx or Rx. No additional metasurface slab would be needed.

The second consideration is efficiency enhancement. The main reason for using metamaterials is to improve the

efficiency for WPT or WEH, when the Rx is not perfectly aligned with the Tx or energy source in a close range. For such a WPT system, the maximum PTE is typically in the range of 50%-60%. Even this level of efficiency can be achieved only when the Tx and Rx are well aligned. On the receiving side or in a WEH system, the DC-RF rectification efficiency is typically about 70%-80% at an optimal power level, as can be observed in Table IV. The efficiency would be much lower under other conditions, especially when the input power level is low. This would make the overall efficiency well below 50%, which is not only a waste of energy, but also a potential health and safety concern that will be addressed in the third design consideration. A few areas need to be further developed to improve the overall efficiency such as better rectifying diodes to improve RF to DC conversion efficiency and a better controlled Tx-Rx coupling. In terms of metamaterials and metasurfaces, design consideration should be given to reducing the loss caused by adding them. Any gain in efficiency achieved by metamaterials should not be canceled out by the additional loss introduced by them. In [184], it has been reported that a simple intermediate magnetic resonant field enhancer can outperform conventional metamaterials, mainly due to the lower added loss.

The third design consideration is the reliability and safety of WTP and WEH systems. There is one of the most notable obstacles for the widespread practical applications of WPT and WEH, especially for a high level of power transfer. A relatively low efficiency as discussed in the previous paragraph means that a significant amount of energy will be either dissipated as heat, which can be a hazard to the WPT system, or radiated into free space, which will cause unintended electromagnetic interferences. For practical applications where the Rx may not be placed in the hotspot area perfectly and aligned well with the Tx. The efficiency would drop even further. For WEH applications, electromagnetic waves as energy harvesting sources may come from different directions with different polarisations at different power levels. The reliability and safety of WPT and WEH systems should be considered very seriously for any real-world applications. To address this, machine learning techniques, such as deep neural networks [91], and reconfigurable intelligent surfaces can be adopted to improve the robustness of WPT and WEH systems.

In previous sections, it has been demonstrated that metamaterials and metasurfaces can help tackle various aspects of WPT and WEH, e.g. high-efficiency long-range power transfer, high power density short-range power transfer, and ambient energy harvesting. For real-world applications, a few practical issues need to be considered as discussed above. At the same time, there are a few attractive emerging and promising future research areas of WPT and WEH based on metamaterials.

A. Simultaneous Wireless Information and Power Transfer

Many functionalities and applications can be envisaged, including but not limited to WPT by harnessing metamaterials for EM fields and waves manipulations [185]. In particular, a unified wireless power and information system would be obtained. Simultaneous wireless information and power transfer (SWIPT) seems to be a feasible solution for future IoT [186]-[188].

For such an application, the challenge on the physical layer employing metamaterials is the development of an energy and information integrated (EII) base station. Compared with existing base stations for wireless communications, an EII base station could offer point-to-point, point-to-multipoint, and specific area power coverage services in addition to mobile network access. The EII base station, which is on the top layer of a SWIPT system, dominates all other devices within a cellular network. These requirements force us to seek out new architecture and design methodology for low-cost and high-efficient EII base stations because WPT is not considered in the traditional base stations.

Programmable metasurfaces (PMS's) and holographic metasurfaces (HMS's) are advanced architectures of metamaterials. PMS was firstly proposed in [189], laying a solid foundation for the following studies. By utilizing digital ideas, a PMS offers a shortcut to integrate EM regulation and digital information. Owning to the discrete phase shift representation method, field programmable gate arrays (FPGAs) are applied directly to manipulate the status of PMS. The low-cost and high-efficiency characteristics of PMS make it possible to realize EII base stations. On the energy transfer aspect, beam-forming and beam-steering techniques performed on PMS indicate that wireless power can be focused in near-field or conveyed to far-field. On the information transfer aspect, PMS can be either viewed as a conventional planar array antenna or treated as a new paradigm of wireless communication [170]. Extensive researches on the above aspects have been conducted, however, studies of energy and information combination on PMS are rarely reported.

Turning now to the middle layer of SWIPT system, in the wireless communication community, reconfigurable intelligent surfaces (RIS) have been discussed in the last two years, as shown in Fig. 24. A relevant overview of studies on metasurfaces as reconfigurable intelligent surfaces in wireless networks supporting SWIPT has been provided in a recent paper [190]. The main features of RIS are hybrid beamforming, signal coverage, and wireless sensing. The prototype of a RIS in the literature is based on PMS. Fundamentals of wireless information and power transfer are overviewed in [191], suggesting that comprehensive researches on prototype design supporting SWIPT should be on the agenda. So far most works on RIS aided SWIPT are contributed by the wireless communication community [192]-[196]. The existing researches mainly focus on model construction and theoretical analysis. Practical hardware platforms of RIS have shown great potentials as a future research direction. SWIPT of intelligent backscatter interpreters could be realized by PMS if energy management is fully considered. Integrating energy and information on PMS for the top and middle layer of SWIPT system involves multi-disciplinary cooperation, which is still an unexploited area.

Another promising hardware architecture for wirelessly powered terminals is the HMS that adopts the holography concept into antenna engineering and communication field [197], [198]. By leveraging the holographic patterning technique on designing metasurfaces, the reference waves and objective waves are interfered with and recorded in the

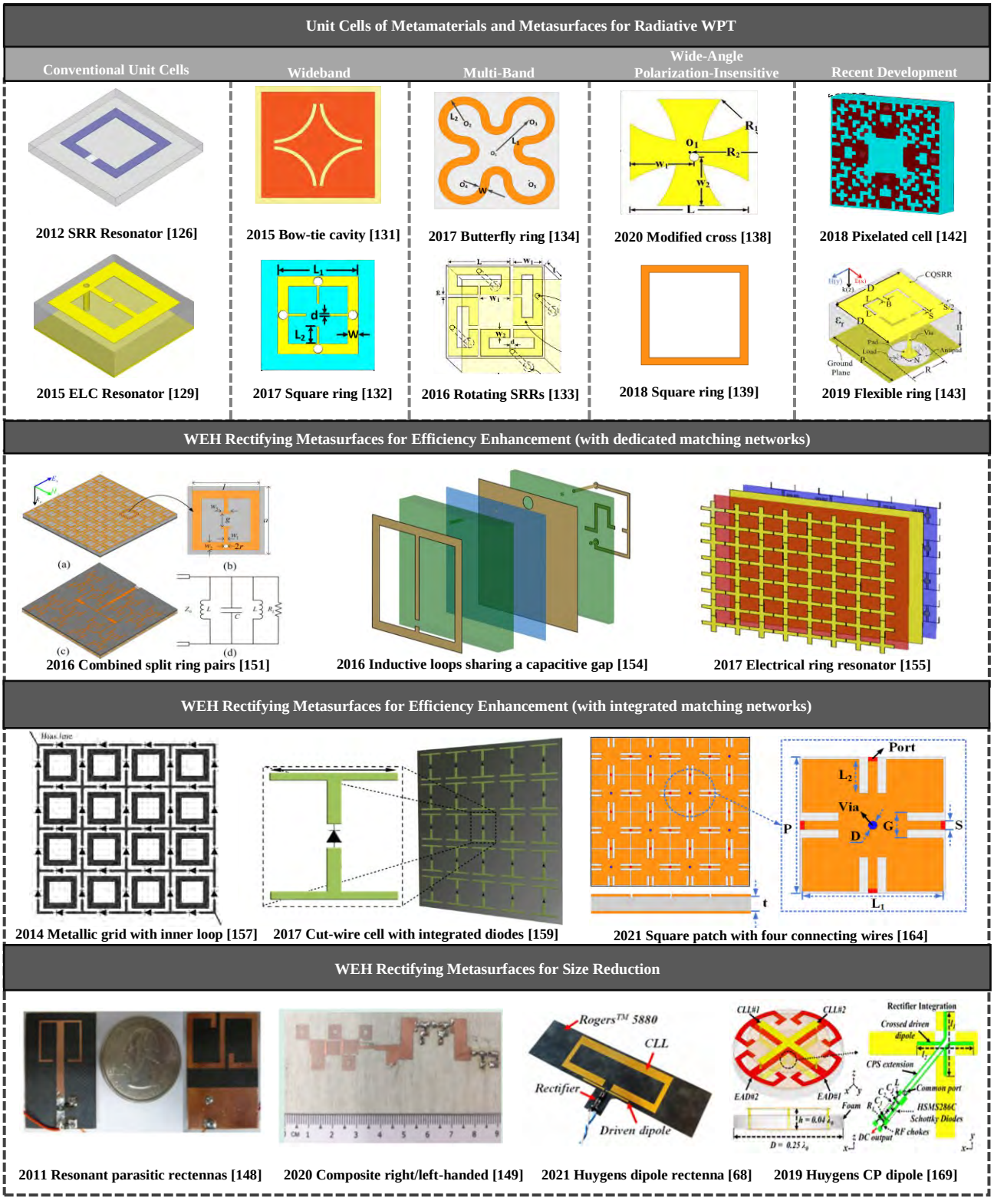

Fig. 23 The research context and the significant progress of metasurface applied to WPT and WEH.

metasurface pattern. Hence, as the reference wave illuminates this pattern, the original wave can be reproduced. In this way, a complicated EM environment can be collected and trained to optimize the metasurface design. More importantly, an HMS has a low profile, low cost, low weight, and high reliability. It worth noting that the holographic principle is feasible for both energy and information transfer. However, a systematic study on this topic is still unavailable. The nature of HMS makes it a good candidate for small-size WPT and RF sensing.

B. Opportunities for near-field WPT

A smart table, as shown in Fig. 25, is a very obvious and highly anticipated device that can benefit from near-field WPT technologies. Multiple electronic devices can be powered on a

wireless charging table. The metasurface can either operate as a Tx itself or as an intermediary to enhance WPT performance between a Tx underneath the table and multiple Rx's on top of the table.

For such applications, it is almost inevitable dynamic control is needed for the operation. The deep neural network can provide an effective way to design metamaterials, as an alternative method to traditional EM-simulation-based approaches [91]. It can potentially be a very useful technique for the design of a smart table in the future, where devices requiring different power levels can be placed on random locations on a smart table.

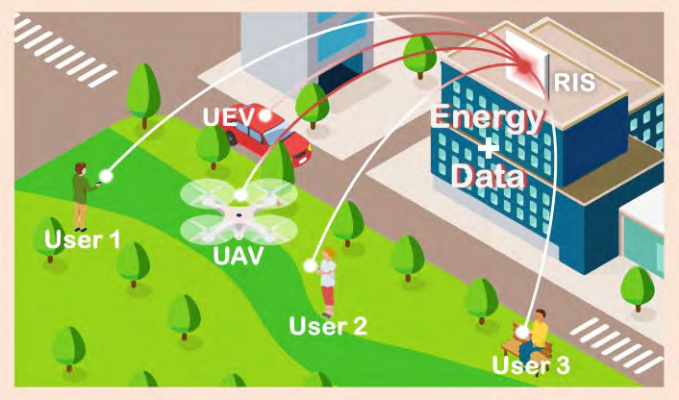

Fig. 24 Conceptual diagram of RIS application scenarios for SWIPT.

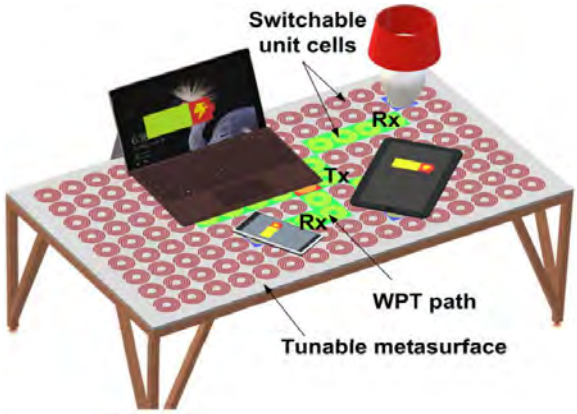

Fig. 25 An artist's rendition of a WPT charging table realized using a tunable metasurface. Multiple receivers on the table can be powered simultaneously. The metasurface dynamically localizes the power into the selected WPT path using switchable and tunable unit cells [91].

Another promising opportunity is chip-level wireless power transfer. To simplify the packaging of integrated circuits and to reduce power consumption associated with data bus cabling, intra-chip and chip-to-chip wireless communications enable high-speed communication at short distances without physical connections[199], [200]. With wireless data bus techniques, a system-on-chip can combine the required electronic circuits of various components and devices onto a single chip. For the measurement and operation of these chips, no wired radio frequency connection is needed to provide input signals or acquire output signals. Nevertheless, a DC power supply is still needed. With chip-level WPT, multiple chips can be placed on a power supplying printed circuit board (PCB), functioning like the smart table shown in Fig. 25.

As shown in Fig. 26, a Tx can be placed either above as a non-contacting testing probe for measurements or below the chip on the PCB as a power supply for the operation of integrated circuit chips. The Rx coil is fabricated on the chip. A metasurface can be utilized to either focus or direct power to where chips are placed. It will make the chip truly wireless. To minimize the die area needed for WPT or SWIPT, millimetre wave or sub-THz WPT techniques can be adapted to provide power wirelessly [200], [201].

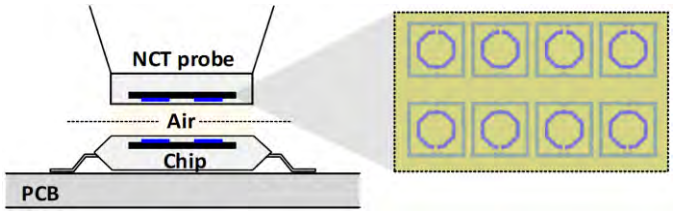

Fig. 26 Wafer-level WPT for the testing and operation of integrated circuit chips [200].

VII. Conclusions

This paper has provided a comprehensive review of the development of metamaterials and metasurfaces for WPT and WEH in recent years. It was shown that for non-radiative applications, metamaterials and metasurfaces have been applied to improve WPT performance with respect to power transfer efficiency and distance. Generally, they were used in three ways: shielding/reflecting, focusing/concentrating, and guiding/ directing. Metamaterials and metasurfaces can reflect EM field in other directions to both suppress unintended EM radiation, and enhance WPT efficiency; Due to their special refractive characteristics, they can concentrate the EM field between a Tx and an Rx, hence improving the WPT efficiency and distance; With dynamic control, they can direct EM field to an Rx especially when the location and power level of the Rx are variable.

For radiative applications, metamaterials and metasurfaces have been widely used in both the radiative near-field (the Fresnel area) and the far-field region. In the near-field region, they have been used as a phased array or a reflective surface to manipulate electromagnetic waves for beamforming purposes.

In the far-field region, metamaterials and metasurfaces are more commonly used for WEH. Far-field WPT and WEH have been compared in detail in this paper. How metamaterials and metasurfaces can improve WEH performance have been reviewed comprehensively. They have been integrated with rectifying circuits to design metamaterial-based rectennas. They can also be used as either parasitic elements or loading components to design metamaterials-assisted rectennas. Either way, they can reduce the circuit size and improve the RF-DC conversion efficiency for WEH. Future development opportunities of metamaterials and metasurfaces for WPT and WEH applications have also been proposed in this paper.

Acknowledgment

We are most grateful for the significant contribution to this paper from Dr. Chaoyun SONG at Heriot-Watt University, UK.

REFERENCES

1 J. Garnica, R. A. Chinga and J. Lin, "Wireless Power Transmission: From Far Field to Near Field," Proceedings of the IEEE, vol. 101, no. 6, pp. 1321-1331, June 2013, doi: 10.1109/JPROC.2013.2251411.

2 S. Y. R. Hui, W. Zhong and C. K. Lee, "A Critical Review of Recent Progress in Mid-Range Wireless Power Transfer," IEEE Transactions on Power Electronics, vol. 29, no. 9, pp. 4500-4511, Sept. 2014, doi: 10.1109/TPEL.2013.2249670.

3 S. Li and C. C. Mi, "Wireless Power Transfer for Electric Vehicle Applications," IEEE Journal of Emerging and Selected Topics in Power Electronics, vol. 3, no. 1, pp. 4-17, March 2015, doi: 10.1109/JESTPE.2014.2319453.

4 Y. Zhuang, A. Chen, C. Xu, Y. Huang, H. Zhao and J. Zhou, "Range-Adaptive Wireless Power Transfer Based on Differential Coupling Using Multiple Bidirectional Coils," IEEE Transactions on Industrial Electronics, vol. 67, no. 9, pp. 7519-7528, Sept. 2020, doi: 10.1109/TIE.2019.2945304.

5 X. Lu, P. Wang, D. Niyato, D. I. Kim and Z. Han, "Wireless Networks With RF Energy Harvesting: A Contemporary Survey," IEEE Communications Surveys & Tutorials, vol. 17, no. 2, pp. 757-789, Secondquarter 2015, doi: 10.1109/COMST.2014.2368999.

6 C. Song, Y. Huang, J. Zhou, J. Zhang, S. Yuan, and P. Carter, "A High-Efficiency Broadband Rectenna for Ambient Wireless Energy Harvesting," IEEE Transactions on Antennas and Propagation, vol. 63, no. 8, pp. 3486-3495, Aug. 2015, doi: 10.1109/TAP.2015.2431719.

7 S. Yuan, Y. Huang, J. Zhou, Q. Xu, C. Song, and P. Thompson, "Magnetic Field Energy Harvesting Under Overhead Power Lines," IEEE Transactions on Power Electronics, vol. 30, no. 11, pp. 6191-6202, Nov. 2015, doi: 10.1109/TPEL.2015.2436702.

8 V. G. Veselago, "The electrodynamics of substances with simultaneously negative values of ε and μ," Sov. Phys. Uspekhi, vol. 10, no. 4, pp. 509–514, Apr. 1968.

9 J. B. Pendry, "Negative refraction makes a perfect lens," Physical review letters 85, pp. 3966, 2000.

10 D. R. Smith, W. J. Padilla, D. C. Vier, S. C. Nemat-Nasser, and S. Schultz, "Composite medium with simultaneously negative permeability and permittivity," Phys. Rev. Lett., vol. 84, no. 18, pp. 4184–4187, Jul. 2002.

11 C. Caloz, T. Itoh, Electromagnetic Metamaterials: Transmission Line Theory and Microwave Applications. Wiley-IEEE Press, New York, USA, 2005.

12 C. L. Holloway, E. F. Kuester, J. A. Gordon, et al., "An overview of the theory and applications of metasurfaces: the two-dimensional equivalents of metamaterials." IEEE Antenna Propagation Mag, vol. 54(2) pp.10-35, 2012.

13 H. T. Chen, A. J. Taylor, N. F. Yu, "A review of metasurfaces: physics and applications," Rep Prog Phys, 79(7):076401, 2016.

14 A. Li, S. Singh and D. Sievenpiper, "Metasurfaces and their applications," Nanophotonics, 7(6), 2018.

15 J. Wang, Y. Li, et al., "Metantenna: when metamaterials meets antenna again," IEEE Trans. Antennas Propagation, 68(3), pp. 1332-1347, 2020.

16 D. Sievenpiper, L. Zhang, R. F. J. Broas, N. G. Alexopolous, E. Yablonovitch, "High-impedance electromagnetic surfaces with a forbidden frequency band," IEEE Trans. Antennas Propagation, 47(11), pp. 2059-2074, 1999

17 J. D Binion, E. Lier, T. H. Hand, et al., "A metamaterial-enabled design enhancing decades-old short backfire antenna technology for space applications." Nat Commun 10, 108 (2019). https://doi.org/10.1038/s41467-018-08032-w

18 Metamaterials electronically scanned array (MESA) radars, https://www.echodyne.com/, accessed in Sep 2021.

19 Kymeta, Metamaterial-Surface Flat-Panel Antenna Technology, 18 June 2019, https://www.kymetacorp.com.

20 Pivotal Commware, https://pivotalcommware.com/m accessed in Sep 2021

21 Metawave, https://www.metawave.co/, accessed in Sep 2021

22 High-Speed Smart Checkpoint System: Evolv Edge, https://www.evolvtechnology.com/, accessed in Sep 2021.

23 Metamaterial Inc. https://metamaterial.com/, accessed in Sep 2021

24 Metaboards Ltd, https://www.metaboards.com/products/, accessed in Sep 2021.

25 Y. Huang, Antennas: from theory to practice, 2nd edition, John Wiley and Sons, Oct. 2021

26 M. N. Hussein, J. Zhou, Y. Huang, M. Kod and A. P. Sohrab, "Frequency Selective Surface Structure Miniaturization Using Interconnected Array Elements on Orthogonal Layers," IEEE Transactions on Antennas and Propagation, vol. 65, no. 5, pp. 2376-2385, May 2017, doi: 10.1109/TAP.2017.2684199.

27 M. N. Hussein, J. Zhou, Y. Huang, M. Kod and A. P. Sohrab, "A Miniaturized Low-Profile Multilayer Frequency-Selective Surface Insensitive to Surrounding Dielectric Materials," IEEE Transactions on Microwave Theory and Techniques, vol. 65, no. 12, pp. 4851-4860, Dec. 2017, doi: 10.1109/TMTT.2017.2709317.

28 M. T. Nguyen, C. V. Nguyen, et al. "Electromagnetic Field Based WPT Technologies for UAVs: A Comprehensive Survey." Electronics 2020, 9, 461. https://doi.org/10.3390/electronics9030461

29 C. T. Rim and C. Mi, Wireless Power Transfer for Electric Vehicles and Mobile Devices, John Wiley & Sons. June 2017, ISBN:9781119329053

30 J. A. Hagerty, F. B. Helmbrecht, W. H. McCalpin, R. Zane and Z. B. Popovic, "Recycling ambient microwave energy with broad-band rectenna arrays," IEEE Transactions on Microwave Theory and Techniques, vol. 52, no. 3, pp. 1014-1024, March 2004, doi: 10.1109/TMTT.2004.823585.

31 E. Donchev, J. S. Pang, P. M. Gammon, et al. "The rectenna device: From theory to practice (a review)." MRS Energy & Sustainability 1, 1(2014). https://doi.org/10.1557/mre.2014.6

32 S. B. Glybovski, S. A. Tretyakov, P. A. Belov, Y. S. Kivshar, and C. R. Simovski, "Metasurfaces: From microwaves to visible," Phys. Rep., vol. 634, pp. 1 – 72, May 2016.

33 A. Sihvola, "Metamaterials in electromagnetics," Metamaterials, vol. 1, no. 1, pp. 2 – 11, Mar. 2007

34 D. R. Smith, J. B. Pendry, and M. C. Wiltshire, "Metamaterials and negative refractive index," Science, vol. 305, no. 5685, pp. 788 – 792, 2004

35 J. Pendry, "Manipulating the near field with metamaterials," Opt. Photon. News, vol. 15, no. 9, pp. 32 – 37, 2004.

36 F. Costa, A. Monorchio, and G. Manara, "Efficient analysis of frequency-selective surfaces by a simple equivalent-circuit model," IEEE Antennas Propag. Mag., vol. 54, no. 4, pp. 35 – 48, Aug. 2012.

37 W. Lee and Y. -K. Yoon, "Wireless Power Transfer Systems Using Metamaterials: A Review," in IEEE Access, vol. 8, pp. 147930-147947, 2020, doi: 10.1109/ACCESS.2020.3015176.

38 Y. Cho et al., "Thin PCB-Type Metamaterials for Improved Efficiency and Reduced EMF Leakage in Wireless Power Transfer Systems," IEEE Transactions on Microwave Theory and Techniques, vol. 64, no. 2, pp. 353-364, Feb. 2016, doi: 10.1109/TMTT.2015.2514090.

39 H. Kim et al., "Coil Design and Measurements of Automotive Magnetic Resonant Wireless Charging System for High-Efficiency and Low Magnetic Field Leakage," IEEE Transactions on Microwave Theory and Techniques, vol. 64, no. 2, pp. 383-400, Feb. 2016, doi: 10.1109/TMTT.2015.2513394.

40 H.-D. Lang, A. Ludwig, and C. D. Sarris, "Convex optimization of wireless power transfer systems with multiple Txs," IEEE Trans. Antennas Propag., vol. 62, no. 9, pp. 4623 – 4636, Sep. 2014.

41 H. Lang and C. D. Sarris, "Semidefinite Relaxation-Based Optimization of Multiple-Input Wireless Power Transfer Systems," IEEE Transactions on Microwave Theory and Techniques, vol. 65, no. 11, pp. 4294-4306, Nov. 2017, doi: 10.1109/TMTT.2017.2696948.

42 H. Lang and C. D. Sarris, "Optimization of Wireless Power Transfer Systems Enhanced by Passive Elements and Metasurfaces," IEEE Transactions on Antennas and Propagation, vol. 65, no. 10, pp. 5462-5474, Oct. 2017, doi: 10.1109/TAP.2017.2735452.

43 C. Lu et al., "Investigation of Negative and Near-Zero Permeability Metamaterials for Increased Efficiency and Reduced Electromagnetic Field Leakage in a Wireless Power Transfer System," IEEE Transactions on Electromagnetic Compatibility, vol. 61, no. 5, pp. 1438-1446, Oct. 2019, doi: 10.1109/TEMC.2018.2865520.

44 S. Kim, H. Park, J. Kim, J. Kim and S. Ahn, "Design and Analysis of a Resonant Reactive Shield for a Wireless Power Electric Vehicle," IEEE Transactions on Microwave Theory and Techniques, vol. 62, no. 4, pp. 1057-1066, April 2014, doi: 10.1109/TMTT.2014.2305404.

45 S. C. Tang, S. Y. Hui, and H. S.-H. Chung, "Evaluation of the shielding effects on printed-circuit-board transformers using ferrite plates and copper sheets," IEEE Trans. Power Electron., vol. 17, no. 6, pp. 1080 – 1088, Nov. 2002.

46 J. Besnoff, M. Chabalko, and D. S. Ricketts, "A frequency-selective zeropermeability metamaterial shield for reduction of near-field electromagnetic energy," IEEE Antennas Wireless Propag. Lett., vol. 15, pp. 654 – 657, Aug. 2016.

47 S. Zhu, C. Zhao, Z. Huang, Y. Zhang and X. Luo, "Enhancement of Wireless

Power Transmission Based on Side-Positioned Metamaterials," 2018 IEEE PES Asia-Pacific Power and Energy Engineering Conference (APPEEC), 2018, pp. 241-245, doi: 10.1109/APPEEC.2018.8566376.
48 C. Lu, X. Huang, X. Tao, C. Rong and M. Liu, "Comprehensive Analysis of Side-Placed Metamaterials in Wireless Power Transfer System," IEEE Access, vol. 8, pp. 152900-152908, 2020, doi: 10.1109/ACCESS.2020.3017492.
49 S. Maji, S. Sinha, B. Regensburger, F. Monticone and K. K. Afridi, "Reduced-Fringing-Field Multi-MHz Capacitive Wireless Power Transfer System Utilizing a Metasurface-based Coupler," 2020 IEEE 21st Workshop on Control and Modeling for Power Electronics (COMPEL), 2020, pp. 1-6, doi: 10.1109/COMPEL49091.2020.9265739.
50 B. Wang, K. H. Teo, T. Nishino, W. Yerazunis, J. Barnwell, and J. Zhang , "Experiments on wireless power transfer with metamaterials" , Applied Physics Letters 98, 254101 (2011) https://doi.org/10.1063/1.3601927
51 A. Ranaweera, Thuc Phi Duong, and Jong-Wook Lee , "Experimental investigation of compact metamaterial for high efficiency mid-range wireless power transfer applications" , Journal of Applied Physics 116, 043914 (2014) https://doi.org/10.1063/1.4891715
52 C. Gu, X. Zhang, "A novel structure of left-handed material with equal magnetic and electric resonant frequency." IEEE Trans. Magn., 53 (6) (2017),
53 J. Prat-Camps, C. Navau, A. Sanche, "Experimental realization of magnetic energy concentration and transmission at a distance by metamaterials." Appl. Phys. Lett., 105 (23) (2014), 234101.
54 D. Huang, Y. Urzhumov, D. R. Smith, K. H. Teo, J. Zhang, "Magnetic superlens-enhanced inductive coupling for wireless power transfer". J. Appl. Phys., 111 (6) (2012).
55 Y. Fan, L. Li, S. Yu, C. Zhu, C. Liang, "Experimental study of efficient wireless power transfer system integrating with highly sub-wavelength metamaterials." Prog. Electromagn. Res., 141 (2013), 769 – 784.
56 D. Ahn, M. Kiani, M. Ghovanloo, "Enhanced wireless power transmission using strong paramagnetic response." IEEE Trans. Magn., 50 (3) (2014), 96 – 103.
57 T. K. Oh, B. Lee, "Analysis of wireless power transfer using metamaterial slabs made of ring resonators at 13.56 MHz." J. Electromagn. Eng. Sci., 13 (4) (2013), 259 – 262
58 S. Li, F. Sun, D. An and S. He, "Increasing Efficiency of a Wireless Energy Transfer System by Spatial Translational Transformation," IEEE Transactions on Power Electronics, vol. 33, no. 4, pp. 3325-3332, April 2018, doi: 10.1109/TPEL.2017.2703591.
59 D. Brizi, N. Fontana, S. Barmada and A. Monorchio, "An Accurate Equivalent Circuit Model of Metasurface-Based Wireless Power Transfer Systems," IEEE Open Journal of Antennas and Propagation, vol. 1, pp. 549-559, 2020, doi: 10.1109/OJAP.2020.3028297.
60 Y. Urzhumov, & D. Smith, "Metamaterial-Enhanced Coupling between Magnetic Dipoles for Efficient Wireless Power Transfer." Physical Review B - PHYS REV B. 83.2011, DoI: 10.1103/PhysRevB.83.205114.
61 H. Younesiraad, M. Bemani, "Analysis of coupling between magnetic dipoles enhanced by metasurfaces for wireless power transfer efficiency improvement." Sci Rep 8, 14865 (2018). https://doi.org/10.1038/s41598-018-33174-8
62 V. R. Gowda, O. Yurduseven, G. Lipworth, T. Zupan, M. S. Reynolds and D. R. Smith, "Wireless Power Transfer in the Radiative Near Field," IEEE Antennas and Wireless Propagation Letters, vol. 15, pp. 1865-1868, 2016, doi: 10.1109/LAWP.2016.2542138.
63 Y. Cho, S. Lee, S. Jeong, et al. "Hybrid metamaterial with zero and negative permeability to enhance efficiency in wireless power transfer system", 2016 IEEE Wireless Power Transfer Conf. (WPTC), 2016, 1 – 3.
64 Y. Cho et al., "Thin Hybrid Metamaterial Slab With Negative and Zero Permeability for High Efficiency and Low Electromagnetic Field in Wireless Power Transfer Systems," IEEE Transactions on Electromagnetic Compatibility, vol. 60, no. 4, pp. 1001-1009, Aug. 2018, doi: 10.1109/TEMC.2017.2751595.
65 S. Pham, T., Kumara Ranaweera, A., Dinh Lam, V., and Lee, J.-W., "Experiments on localized wireless power transmission using a magneto-inductive wave two-dimensional metamaterial cavity", Applied Physics Express, vol. 9, no. 4, p. 044101, 2016. doi:10.7567/APEX.9.044101.
66 C. Pfeiffer and A. Grbic, "Metamaterial Huygens' surfaces: Tailoring wave fronts with reflectionless sheets," Phys. Rev. Lett., vol. 110, no. 19,May 2013, Art. no. 197401.
67 W. Lin and R. W. Ziolkowski, "Electrically Small Huygens Antenna-Based Fully-Integrated Wireless Power Transfer and Communication System," IEEE Access, vol. 7, pp. 39762-39769, 2019, doi: 10.1109/ACCESS.2019.2903545.
68 W. Lin and R. W. Ziolkowski, "Electrically Small, Single-Substrate Huygens Dipole Rectenna for Ultracompact Wireless Power Transfer Applications," IEEE Transactions on Antennas and Propagation, vol. 69, no. 2, pp. 1130-1134, Feb. 2021, doi: 10.1109/TAP.2020.3004987.
69 H. Younesiraad, M. Bemani and L. Matekovits, "Optimal Huygens' Metasurface for Wireless Power Transfer Efficiency Improvement," IEEE Access, vol. 8, pp. 216409-216418, 2020, doi: 10.1109/ACCESS.2020.3041337.
70 R. Das, A. Basir and H. Yoo, "A Metamaterial-Coupled Wireless Power Transfer System Based on Cubic High-Dielectric Resonators," IEEE Transactions on Industrial Electronics, vol. 66, no. 9, pp. 7397-7406, Sept. 2019, doi: 10.1109/TIE.2018.2879310.
71 T. Shaw and D. Mitra, "Design of miniaturized low-loss and flexible multi-band metamaterial for microwave application", Appl. Phys. A, vol. 124, no. 4, 2018.
72 T. Shaw and D. Mitra, "Wireless Power Transfer System Based on Magnetic Dipole Coupling With High Permittivity Metamaterials," IEEE Antennas and Wireless Propagation Letters, vol. 18, no. 9, pp. 1823-1827, Sept. 2019, doi: 10.1109/LAWP.2019.2930769.
73 D. Brizi, J. P. Stang, A. Monorchio and G. Lazzi, "A Compact Magnetically Dispersive Surface for Low-Frequency Wireless Power Transfer Applications," IEEE Transactions on Antennas and Propagation, vol. 68, no. 3, pp. 1887-1895, March 2020, doi: 10.1109/TAP.2020.2967320.
74 L. Li, H. Liu, H. Zhang and W. Xue, "Efficient Wireless Power Transfer System Integrating With Metasurface for Biological Applications," IEEE Transactions on Industrial Electronics, vol. 65, no. 4, pp. 3230-3239, April 2018, doi: 10.1109/TIE.2017.2756580.
75 D. Brizi, N. Fontana, M. Tucci, S. Barmada and A. Monorchio, "A Spiral Resonators Passive Array for Inductive Wireless Power Transfer Applications With Low Exposure to Near Electric Field," IEEE Transactions on Electromagnetic Compatibility, vol. 62, no. 4, pp. 1312-1322, Aug. 2020, doi: 10.1109/TEMC.2020.2991123.
76 M. Wang et al., "Broadband Implantable Antenna for Wireless Power Transfer in Cardiac Pacemaker Applications," IEEE Journal of Electromagnetics, RF and Microwaves in Medicine and Biology, vol. 5, no. 1, pp. 2-8, March 2021, doi: 10.1109/JERM.2020.2999205.
77 F. Zhang, S. Hackworth, W. Fu, and M. Sun, "The relay effect on wireless power transfer using witricity," Proc. IEEE Conf. Electromagn. Field Comput., May 9 – 12, 2010, Chicago, US.
78 W. X. Zhong, C. K. Lee and S. Y. Hui, "Wireless power domino-resonator systems with noncoaxial axes and circular structures," IEEE Transactions on Power Electronics, vol. 27, no. 11, pp. 4750-4762, Nov. 2012, doi:10.1109/TPEL.2011.2174655.
79 C. Saha, I. Anya, C. Alexandru, and R. Jinks , "Wireless power transfer using relay resonators" , Applied Physics Letters 112, 263902 (2018) https://doi.org/10.1063/1.5022032
80 C. Xu, Y. Zhuang, C. Song, Y. Huang and J. Zhou, "Dynamic Wireless Power Transfer System With an Extensible Charging Area Suitable for Moving Objects," IEEE Transactions on Microwave Theory and Techniques, vol. 69, no. 3, pp. 1896-1905, March 2021, doi: 10.1109/TMTT.2020.3048337.
81 I. Khromova and C. J. Stevens, "Harnessing Magneto-inductive Waves for Wireless Power Transfer," 2018 IEEE Wireless Power Transfer Conference (WPTC), 2018, pp. 1-3, doi: 10.1109/WPT.2018.8639243.
82 A.L.A.K.Ranaweera, T.S.Pham, H.N. Bui, et al. "An active metasurface for field-localizing wireless power transfer using dynamically reconfigurable cavities." Sci Rep 9, 11735 (2019). https://doi.org/10.1038/s41598-019-48253-7
83 A. Rahman, P. A. Belov, M. G. Silveirinha, C. R. Simovski,Y. Hao, and C. Parini, "The importance of Fabry – Perot resonance and the role of shielding in subwavelength imaging performance of multiwire endoscopes", Appl. Phys. Lett. 94, 031104 (2009).
84 P. A. Belov, G. K. Palikaras, Y. Zhao, A. Rahman, C. R. Simovski, Y. Hao, and C. Parini, "Experimental demonstra tion of multiwire endoscopes capable of manipulating near fields with subwavelength resolution", Appl. Phys. Lett. 97, 191905 (2010).
85 M. Song, K. Baryshnikova, A. Markvart et.al. "Smart Table Based on a Metasurface for Wireless Power Transfer", Physical Review Applied, vol.11 pp.054046, 2019,
DOI: 10.1103/physrevapplied.11.054046
86 M. Song, P. Belov, and P. Kapitanova, Wireless power transfer based on dielectric resonators with colossal permittivity, Appl. Phys. Lett. 109, 223902 (2016)
87 M. Song, P. Belov and P. Kapitanova, "Metasurface for Wireless Power

Transfer to Multiple Receivers," 2019 IEEE International Conference on Microwaves, Antennas, Communications and Electronic Systems (COMCAS), 2019, pp. 1-2, doi: 10.1109/COMCAS44984.2019.8958292.

88 F. Liu, P. Jayathurathnage and S. A. Tretyakov, "Active Metasurfaces as a Platform for Capacitive Wireless Power Transfer Supporting Multiple Receivers," 2019 Thirteenth International Congress on Artificial Materials for Novel Wave Phenomena (Metamaterials), 2019, pp. X-227-X-229, doi: 10.1109/MetaMaterials.2019.8900808.

89 Y. Zhao, C. Huang, Z. Song, C. Yu, S. Liang, X. Luo, and A. Qing, "A digital metamaterial of arbitrary base based on voltage tunable liquid crystal," IEEE Access, vol. 7, pp. 79671 – 79676, Jul. 2019.

90 W. Wang, C. Xu, M. Yan, A. Wang, J. Wang, M. Feng, J. Wang, and S. Qu, "Broadband tunable metamaterial absorber based on U-shaped ferrite structure," IEEE Access, vol. 7, pp. 150969 – 150975, Oct. 2019.

91 H. N. Bui, J. -S. Kim and J. -W. Lee, "Design of Tunable Metasurface Using Deep Neural Networks for Field Localized Wireless Power Transfer," IEEE Access, vol. 8, pp. 194868-194878, 2020, doi: 10.1109/ACCESS.2020.3033527.

92 Z. Liu, D. Zhu, S. P. Rodrigues, K.-T. Lee, and W. Cai, ''Generative model for the inverse design of metasurfaces,'' Nano Lett., vol. 18, no. 10, pp. 6570–6576, Sep. 2018.

93 E. S. Harper, E. J. Coyle, J. P. Vernon, and M. S. Mills, ''Inverse design of broadband highly reflective metasurfaces using neural networks,'' Phys. Rev. B, Condens. Matter, vol. 101, no. 19, May 2020, Art. no. 195104.

94 W. Ma, F. Cheng, Y. Xu, Q. Wen, and Y. Liu, ''Probabilistic representation and inverse design of metamaterials based on a deep generative model with semi-supervised learning strategy,'' Adv. Mater., vol. 31, no. 35, Aug. 2019, Art. no. 1901111

95 W. C. Brown, "The history of power transmission by radio waves," IEEE Trans. Microwave Theory Tech., vol. 32, pp. 1230–1242, Sep. 1984.

96 J. Sherman, Iii, "Properties of focused apertures in the Fresnel region," IRE Trans. Antennas Propag., vol. 10, no. 4, pp. 399-408, Jul. 1962.

97 R. C. Hansen, "Focal region characteristics of focused array antennas," IEEE Trans. Antennas Propag., vol. 33, no. 12, pp. 1328-1337, Dec. 1985.

98 J. Durnin, M. J. Jr, and J. H. Eberly. "Diffraction-free beams," Phys. Rev. Lett., vol. 58, no. 15, pp. 1499-1501, 1987.

99 L. Shafai, A. A. Kishk, and A. Sebak, "Near field focusing of apertures and reflector antennas," WESCANEX 97: Communications, Power and Computing. Conference Proceedings, Winnipeg, MB, Canada, 2002, pp. 246-251.

100 J. Bor, S. Clauzier, and O. Lafond, et al., "60 GHz foam-based antenna for near-field focusing," Electron. Lett., vol. 50, no. 8, pp. 571-572, 2015.

101 A. Buffi, P. Nepa, and G. Manara, "Design criteria for near-field-focused planar arrays," IEEE Antenn. Propag. Mag., vol. 54, no. 1, pp. 40-50, Feb. 2012.

102 F. Tofigh, J. Nourinia, M. N. Azarmanesh, and K. M. Khazaei, "Near-field focused array microstrip planar antenna for medical applications," IEEE Antennas Wireless Propag. Lett., vol. 13, no. 13, pp. 951-954, May. 2014.

103 R. Siragusa, P. Lemaitre-Auger, and S. Tedjini, "Tunable near-field focused circular phase-array antenna for 5.8-GHz RFID applications," IEEE Antennas Wireless Propag. Lett., vol. 10, no. 1, pp. 33-36, Jan. 2011.

104 K. D. Stephan, J. B. Mead, and D. M. Pozar, et al., "A near field focused microstrip array for a radiometric temperature sensor," IEEE Trans. Antennas Propag., vol. 55, no. 4, pp. 1199-1203, Apr. 2007.

105 S. Karimkashi, and A. A. Kishk, "Focusing properties of Fresnel zone plate lens antennas in the near-field region," IEEE Trans. Antennas Propag., vol. 59, no. 5, pp. 1481-1487, May. 2011.

106 I. V. Minin, and O. V. Minin, Basic principles of Fresnel antenna arrays. Springer Berlin Heidelberg, 2008.

107 A. J. Martínez-Ros, J. L. Gómez-Tornero, and J. Monzó-Cabrera, "Microwave near-field focusing properties of width-tapered microstrip leaky-wave antenna," IEEE Trans. Antennas Propag., vol. 61, no. 6, pp. 2981-2990, Mar, 2013.

108 J. L. Gómez-Tornero, D. Blanco, E. Rajo-Iglesias, and N. Llombart, "Holographic surface leaky-wave lenses with circularly-polarized focused near-fields—part I: concept, design and analysis theory," IEEE Trans. Antennas Propag., vol. 61, no. 7, pp. 3475-3485, Jul. 2013.

109 N. Shinohara, "History and Innovation of Wireless Power Transfer via Microwaves," in IEEE Journal of Microwaves, vol. 1, no. 1, pp. 218-228, winter 2021, doi: 10.1109/JMW.2020.3030896.

110 C. T. Rodenbeck et al., "Microwave and Millimeter Wave Power Beaming," in IEEE Journal of Microwaves, vol. 1, no. 1, pp. 229-259, winter 2021, doi: 10.1109/JMW.2020.3033992.

111 N. Takabayashi, N. Shinohara, T. Mitani, M. Furukawa and T. Fujiwara, "Rectification Improvement With Flat-Topped Beams on 2.45-GHz Rectenna Arrays," in IEEE Transactions on Microwave Theory and Techniques, vol. 68, no. 3, pp. 1151-1163, March 2020, doi: 10.1109/TMTT.2019.2951098.

112 N. Shinohara, "Beam Control Technologies With a High-Efficiency Phased Array for Microwave Power Transmission in Japan," in Proceedings of the IEEE, vol. 101, no. 6, pp. 1448-1463, June 2013, doi: 10.1109/JPROC.2013.2253062.

113 S. Kojima, T. Mitani and N. Shinohara, "Array Optimization for Maximum Beam Collection Efficiency to an Arbitrary Receiving Plane in the Near Field," in IEEE Open Journal of Antennas and Propagation, vol. 2, pp. 95-103, 2021, doi: 10.1109/OJAP.2020.3044443.

114 H. T. Chou, T. M. Hung, and N. N. Wang, et al., "Design of a near-field focused reflectarray antenna for 2.4 GHz RFID reader applications," IEEE Trans. Antennas Propag., vol. 59, no. 3, pp. 1013-1018, Mar. 2011.

115 X. Wu, X. Xia, and J. Tian, et al., "Broadband reflective metasurface for focusing underwater ultrasonic waves with linearly tunable focal length," Appl. Phys. Lett., vol. 108, no. 16, Apr. 2016, Art. no. 163502.

116 S. Zhang, M. H. Kim, and F. Aieta, et al., "High efficiency near diffraction-limited mid-infrared flat lenses based on metasurface reflectarrays," Opt. Express, vol. 24, pp. 18024–18034, Aug. 2016.

117 H. Li, G. Wang, T. Cai, H. Hou, and W. Guo, "Wideband Transparent Beam-Forming Metadevice with Amplitude- and Phase-Controlled Metasurface", Phys. Rev. Applied 11, 014043, 22 Jan. 2019

118 L. Bao et al., "Multi-Beam Forming and Controls by Metasurface With Phase and Amplitude Modulations," in IEEE Transactions on Antennas and Propagation, vol. 67, no. 10, pp. 6680-6685, Oct. 2019, doi: 10.1109/TAP.2019.2925289.

119 M. Boyarsky, T. Sleasman, M. F. Imani, et al., "Electronically steered metasurface antenna". Sci Rep 11, 4693 (2021). https://doi.org/10.1038/s41598-021-83377-9

120 S. Yu, H. Liu, and L. Li, "Design of near-field focused metasurface for high-efficient wireless power transfer with multifocus characteristics," IEEE Trans. Ind. Electron., vol. 66, no. 5, pp. 3993-4002, May. 2019.

121 P. Zhang, L. Li, and X. Zhang et al., "Design, measurement and analysis of near-field focusing reflective metasurface for dual-polarization and multi-focus wireless power transfer," IEEE Access, vol. 7, pp. 110387-110399, Aug. 2019.

122 O. Yurduseven, D. L. Marks, and D. R. Smith et al., "Design and analysis of a reconfigurable holographic metasurface aperture for dynamic focusing in the Fresnel zone," IEEE Access, vol. 5, pp. 15055-15065, Jun. 2017.

123 O. Yurduseven, S. Ye, and D. R. Smith, et al., "3D conductive polymer printed metasurface antenna for Fresnel focusing," Designs, vol. 3, no. 3, pp. 1-4, Sep. 2019.

124 A. A. G. Amer, S. Z. Sapuan, N. Nasimuddin, A. Alphones and N. B. Zinal, "A Comprehensive Review of Metasurface Structures Suitable for RF Energy Harvesting," in IEEE Access, vol. 8, pp. 76433-76452, 2020, doi: 10.1109/ACCESS.2020.2989516.

125 N. I. Landy, S. Sajuyigbe, and D. R. Smith et al., "Perfect metamaterial absorber," Phys. Rev. Lett., vol. 100, May. 2008, Art. no. 207402.

126 O. M. Ramahi, T. S. Almoneef, M. Alshareef, and M. S. Boybay, "Metamaterial particles for electromagnetic energy harvesting," Appl. Phys. Lett., vol. 101, no. 17, Oct. 2012, Art. no. 173903.

127 M. R. Alshareef and O. M. Ramahi, "Electrically small particles combining even- and odd-mode currents for microwave energy harvesting," Appl. Phys. Lett., vol. 104, Jul. 2014, Art. no. 253906.

128 X. Duan, X. Chen, Y. Zhou, L. Zhou, and S. Hao, "Wideband metamaterial electromagnetic energy harvester with high capture efficiency and wide incident angle," IEEE Antennas Wireless Propag. Lett., vol. 17, no. 9, pp. 1617-1621, Sep. 2018.

129 T. S. Almoneef and O. M. Ramahi, "Metamaterial electromagnetic energy harvester with near unity efficiency," Appl. Phys. Lett., vol. 106, no. 15, Apr. 2015, Art. no. 153902.

130 B. Alavikia, T. S. Almoneef, and O. M. Ramahi, "Complementary split-ring resonator arrays for electromagnetic energy harvesting," Appl. Phys. Lett., vol. 107, no. 3, pp. 1-6, 2015.

131 B. Alavikia, T. S. Almoneef, and O. M. Ramahi, "Wideband resonator arrays for electromagnetic energy harvesting and wireless power transfer," Appl. Phys. Lett., vol. 107, no. 24, Dec. 2015, Art. no. 243902.

132 H. T. Zhong, X. X. Yang, X. T. Song, Z. Y. Guo, and F. Yu, "Wideband metamaterial array with polarization-independent and wide incident angle for harvesting ambient electromagnetic energy and wireless power transfer," Appl. Phys. Lett., vol. 111, no. 21, Nov. 2017, Art. no. 213902.

133 H. T. Zhong, X. X. Yang, C. Tan, and K. Yu, "Triple-band polarization-insensitive and wide-angle metamaterial array for electromagnetic energy

harvesting," Appl. Phys. Lett., vol. 109, no. 25, Dec. 2016, Art. no. 253904.
134 X. Zhang, H. Liu, and L. Li, "Tri-band miniaturized wide-angle and polarization-insensitive metasurface for ambient energy harvesting," Appl. Phys. Lett., vol. 111, no. 7, Aug. 2017, Art. no. 071902.
135 E. Karakaya, F. Bagci, A. E. Yilmaz, and B. Akaoglu, "Metamaterial-based four-band electromagnetic energy harvesting at commonly used GSM and Wi-Fi frequencies," J. Electron. Mater., vol. 48, no. 4, pp. 2307-2316, Apr. 2019.
136 E. Karakaya, F. Bagci, S. Can, A. E. Yilmaz, and B. Akaoglu, "Four-band electromagnetic energy harvesting with a dual-layer metamaterial structure," Int. J. RF Microw. Comput. Eng., vol. 29, no. 1, pp. 1-7, Nov. 2018.
137 S. Shang, S. Yang, J. Liu, M. Shan, and H. Cao, "Metamaterial electromagnetic energy harvester with high selective harvesting for left- and right-handed circularly polarized waves," J. Appl. Phys., vol. 120, no. 4, Jul. 2016, Art. no. 045106.
138 F. Yu, X. Yang, H. Zhong, C. Chu, and S. Gao, "Polarization-insensitive wide-angle-reception metasurface with simplified structure for harvesting electromagnetic energy," Appl. Phys. Lett., vol. 113, no. 12, Sep. 2018, Art. no. 123903.
139 X. Zhang, H. Liu, and L. Li, "Electromagnetic power harvester using wide-angle and polarization-insensitive metasurfaces," Appl. Sci., vol. 8, no. 4, Mar. 2018, Art. no. 497.
140 F. Yu, G. Q. He, X. X. Yang, J. Du, and S. Gao, "Polarization-insensitive metasurface for harvesting electromagnetic energy with high efficiency and frequency stability over wide range of incidence angles," Appl. Sci., vol. 10, no. 22, Nov. 2020, Art. no. 8047.
141 B. Alavikia, T. S. Almoneef, and O. M. Ramahi, "Complementary split ring resonator arrays for electromagnetic energy harvesting," Appl. Phys. Lett., vol. 107, no. 3, Jul. 2015, Art. no. 033902.
142 B. Ghaderi, V. Nayyeri, M. Soleimani, and O. M. Ramahi, "Pixelated metasurface for dual-band and multi-polarization electromagnetic energy harvesting," Sci. Rep., vol. 8, no. 1, pp. 1-12, Dec. 2018.
143 A. Ghaneizadeh, K. Ma_nezhad, and M. Joodaki, "Design and fabrication of a 2D-isotropic flexible ultra-thin metasurface for ambient electromagnetic energy harvesting," AIP Adv., vol. 9, no. 2, Feb. 2019, Art. no. 025304.
144 W. Hu, Z. Yang, F. Zhao, G. Wen, J. Li, Y. Huang, D. Inserra, and Z. Chen, "Low-cost air gap metasurface structure for high absorption efficiency energy harvesting," Int. J. Antennas Propag., vol. 2019, pp. 1-8, Sep. 2019.
145 M. A. Aldhaeebi, T. S. Almoneef, "Planar dual polarized metasurface array for microwave energy harvesting," Electronics, vol. 9, no. 12, Nov. 2020, Art. no. 1985.
146 A. M. Hawkes, A. R. Katko, and S. A. Cummer, "A microwave metamaterial with integrated power harvesting functionality," Appl. Phys. Lett., vol. 103, no. 16, Oct. 2013, Art. no. 163901.
147 R. Ashtari, M. Baginski, and R. Dean, "A 2.45-GHz frequency-selective rectenna for wireless energy harvesting," Microw. Opt. Technol. Lett., vol. 58, pp. 2508-2512, Mar. 2016.
148 N. Zhu, R. W. Ziolkowskia, and H Xin, "A metamaterial-inspired, electrically small rectenna for high-efficiency, low power harvesting and scavenging at the global positioning system L1 frequency," Appl. Phys. Lett., vol. 99, Sep. 2011, Art. no. 114101.
149 K. T. Chandrasekaran, K. Agarwal, and Nasimuddin, et al., "Compact dual-band metamaterial-based high-efficiency rectenna: an application for ambient electromagnetic energy harvesting," IEEE Antennas Propag. Mag., vol. 62, no. 3, pp. 18-29, Jun. 2020.
150 D. Ferreira, L. Sismeiro, and A. Ferreira, et al., "Hybrid FSS and rectenna design for wireless power harvesting," IEEE Trans. Antennas Propag., vol. 64, no. 5, pp. 2038-2042, May. 2016.
151 P. Xu, S. Y. Wang, and W. Geyi, "Design of an effective energy receiving adapter for microwave wireless power transmission application," AIP Adv., vol. 6, no. 10, Oct. 2016, Art. no. 105010.
152 T. S. Almoneef, F. Erkmen, and O. M. Ramahi, "Harvesting the energy of multi-polarized electromagnetic waves," Sci. Rep., vol. 7, Dec. 2017, Art. no. 14656.
153 M. El Badawe, O. M. Ramahi, "Efficient metasurface rectenna for electromagnetic wireless power transfer and energy harvesting," Prog. Electromagn. Res., vol. 161, pp. 35–40, Mar. 2018.
154 X. Duan, X. Chen, and L. Zhou, "A metamaterial electromagnetic energy rectifying surface with high harvesting efficiency," AIP Adv., vol. 6, no. 12, Dec. 2016, Art. no. 125020.
155 M. El Badawe, T. S. Almoneef, and O. M. Ramahi, "A metasurface for conversion of electromagnetic radiation to DC," AIP Adv., vol. 7, no. 3, Mar. 2017, Art. no. 035112.
156 F. Erkmen, T. S. Almoneef and O. M. Ramahi, "Scalable electromagnetic energy harvesting using frequency-selective surfaces," IEEE Trans. Microwave Theory Tech., vol. 66, no. 5, pp. 2433-2441, May. 2018.
157 S. Keyrouz, G. Perotto, and H. J. Visser, "Frequency selective surface for radio frequency energy harvesting applications," IET Microw. Antennas Propag., vol. 8, no. 7, pp. 523–531, May. 2014.
158 R. Wang, D. Ye, and S. Dong et al., "Optimal matched rectifying surface for space solar power satellite applications, " IEEE Trans. Microwave Theory Tech., vol. 62, no. 4, pp. 1080-1089, Apr. 2014.
159 G. T. Oumbé Tékam, V. Ginis, and J. Danckaert et al., "Designing an efficient rectifying cut-wire metasurface for electromagnetic energy harvesting," Appl. Phys. Lett., vol. 110, Feb. 2017, Art. no. 083901.
160 T. S. Almoneef, F. Erkmen, M. A. Alotaibi and O. M. Ramahi, "A new approach to microwave rectennas using tightly coupled antennas," IEEE Trans. Antennas Propag., vol. 66, no. 4, pp. 1714-1724, Apr. 2018.
161 A. Z. Ashoor, T. S. Almoneef and O. M. Ramahi, "A planar dipole array surface for electromagnetic energy harvesting and wireless power transfer," IEEE Trans. Microwave Theory Tech., vol. 66, no. 3, pp. 1553-1560, Mar. 2018.
162 A. Z. Ashoor and O. M. Ramahi, "Polarization-independent cross-dipole energy harvesting surface," IEEE Trans. Microwave Theory Tech., vol. 67, no. 3, pp. 1130-1137, Mar. 2019.
163 M. A. Aldhaeebi and T. S. Almoneef, "Highly efficient planar metasurface rectenna," IEEE Access, vol. 8, pp. 214019-214029, Nov. 2020.
164 L. Li, X. Zhang, and Y. Huang et al., "Compact dual-band, wide-angle, polarization-angle-independent rectifying metasurface for ambient energy harvesting and wireless power transfer," IEEE Trans. Microwave Theory Tech., vol. 69, no. 3, pp. 1518-1528, Mar. 2021.
165 L. Li, X. Zhang, C. Song, W. Zhang, T. Jia and Y. Huang, "Compact Dual-Band, Wide-Angle, Polarization- Angle -Independent Rectifying Metasurface for Ambient Energy Harvesting and Wireless Power Transfer," IEEE Transactions on Microwave Theory and Techniques, vol. 69, no. 3, pp. 1518-1528, March 2021.
166 C. Song, Y. Huang, J. Zhou, P. Carter, S. Yuan, Q. Xu and Z. Fei, "Matching network elimination in broadband rectennas for high-efficiency wireless power transfer and energy harvesting," IEEE Trans. Industrial Electronics, vol. 64, no. 5, pp. 3950–3961, Apr. 2017.
167 N. Zhu, R. W. Ziolkowski and H. Xin, "Electrically Small GPS L1 Rectennas," IEEE Antennas and Wireless Propagation Letters, vol. 10, pp. 935-938, 2011.
168 W. Lin and R. W. Ziolkowski, "Electrically Small Huygens CP Rectenna With a Driven Loop Element Maximizes Its Wireless Power Transfer Efficiency," IEEE Transactions on Antennas and Propagation, vol. 68, no. 1, pp. 540-545, Jan. 2020.
169 W. Lin, R. W. Ziolkowski and J. Huang, "Electrically Small, Low-Profile, Highly Efficient, Huygens Dipole Rectennas for Wirelessly Powering Internet-of-Things Devices," IEEE Transactions on Antennas and Propagation, vol. 67, no. 6, pp. 3670-3679, June 2019.
170 G. Liu, L. Li, and J. Han, et al., "Frequency-domain and spatial-domain reconfigurable metasurface," ACS Appl. Mater. Interfaces, vol. 12, no. 20, pp. 23554-23564, Apr. 2020.
171 J. Han, L. Li, H. Yi, et al., "Versatile orbital angular momentum vortex beam generator based on reconfigurable reflective metasurface," Jpn. J. Appl. Phys., vol. 57, Oct. 2018, Art. no. 120303.
172 T. J. Cui, M. Q. Qi, and X. Wan, et al., "Coding metamaterials, digital metamaterials and programming metamaterials," Light Sci. Appl., vol. 3, 2014.
173 L. Zhang, X. Q. Chen, and S. Liu, et al., "Space-time-coding digital metasurfaces," Nat. Commun., vol. 9, Oct. 2018, Art. no. 4334.
174 Q. Ma, G. Bai, and H. Jing, et al., "Smart metasurface with self-adaptively reprogrammable functions," Light Sci. Appl., vol. 8, no. 98, pp. 1-12, 2019.
175 R. F. Harrington and J. R. Mautz, "Theory of characteristic modes for conducting bodies," IEEE Trans. Antennas Propag., vol. AP-19, no. 5, pp. 622–628, Sep. 1971.
176 R. Harrington and J. Mautz, "Computation of characteristic modes for conducting bodies," IEEE Trans. Antennas Propag., vol. AP-19, no. 5, pp. 629–639, Sep. 1971.
177 Y. Chen and C.-F. Wang, Characteristic Modes: Theory and Applications in Antenna Engineering. Hoboken, NJ, USA: Wiley, 2015.
178 W. Zhang, C. Song, R. Pei, Y. Huang and J. Zhou, "Broadband Metasurface Antenna Using Hexagonal Loop-Shaped Unit Cells," in IEEE Access, vol. 8, pp. 223797-223805, 2020, doi: 10.1109/ACCESS.2020.3043656.
179 K. Lee, S. K. Hong, "Rectifying metasurface with high efficiency at low power for 2.45 GHz band," IEEE Antennas Wireless Propag. Lett., vol. 19, no. 12, pp. 2216-2220, Dec. 2020.
180 F. H. Lin and Z. N. Chen, "Truncated Impedance Sheet Model for Low-Profile Broadband Nonresonant-Cell Metasurface Antennas Using

Characteristic Mode Analysis," in IEEE Transactions on Antennas and Propagation, vol. 66, no. 10, pp. 5043-5051, Oct. 2018, doi: 10.1109/TAP.2018.2854366.
181 T. Li et al., "Characteristic Mode Inspired Dual-Polarized Double-Layer Metasurface Lens," in IEEE Transactions on Antennas and Propagation, vol. 69, no. 6, pp. 3144-3154, June 2021, doi: 10.1109/TAP.2020.3046423.
182 K. Niotaki, A. Collado, and A. Georgiadis, et al., "Solar/electromagnetic energy harvesting and wireless power transmission," Proc. IEEE, vol. 102, no. 11, pp. 1712-1722, Nov. 2014.
183 Y. K. Tan and S. K. Panda, "Energy harvesting from hybrid indoor ambient light and thermal energy sources for enhanced performance of wireless sensor nodes," IEEE Trans. Ind. Electron., vol. 58, no. 9, pp. 4424-4435, Sep. 2011.
184 M. J. Chabalko, J. Besnoff and D. S. Ricketts, "Magnetic Field Enhancement in Wireless Power With Metamaterials and Magnetic Resonant Couplers," in IEEE Antennas and Wireless Propagation Letters, vol. 15, pp. 452-455, 2016, doi: 10.1109/LAWP.2015.2452216.
185 Ma, Q., Cui, T.J. "Information Metamaterials: bridging the physical world and digital world," PhotoniX, vol. 1, no. 1, (2020).
186 B. Clerckx, R. Zhang, R. Schober, D. W. K. Ng, D. I. Kim and H. V. Poor, "Fundamentals of Wireless Information and Power Transfer: From RF Energy Harvester Models to Signal and System Designs," IEEE Journal on Selected Areas in Communications, vol. 37, no. 1, pp. 4-33, Jan. 2019.
187 S. Bi, C. K. Ho and R. Zhang, "Wireless powered communication: opportunities and challenges," IEEE Communications Magazine, vol. 53, no. 4, pp. 117-125, April 2015.
188 W. Ejaz, M. Naeem, A. Shahid, A. Anpalagan and M. Jo, "Efficient Energy Management for the Internet of Things in Smart Cities," IEEE Communications Magazine, vol. 55, no. 1, pp. 84-91, January 2017.
189 T. Cui, M. Qi, X. Wan, et al. "Coding metamaterials, digital metamaterials and programmable metamaterials." Light Sci Appl 3, e218 (2014).
190 A. A. Eteng, H. H. Goh, S. K. A. Rahim and A. Alomainy, "A Review of Metasurfaces for Microwave Energy Transmission and Harvesting in Wireless Powered Networks," in IEEE Access, vol. 9, pp. 27518-27539, 2021, doi: 10.1109/ACCESS.2021.3058151.
191 W. Tang et al., "Wireless Communications with Programmable Metasurface: New Paradigms, Opportunities, and Challenges on Transceiver Design," IEEE Wireless Communications, vol. 27, no. 2, pp. 180-187, April 2020.
192 C. Pan et al., "Intelligent Reflecting Surface Aided MIMO Broadcasting for Simultaneous Wireless Information and Power Transfer," in IEEE Journal on Selected Areas in Communications, vol. 38, no. 8, pp. 1719-1734, Aug. 2020, doi: 10.1109/JSAC.2020.3000802.
193 H. Yang, X. Yuan, J. Fang and Y. -C. Liang, "Reconfigurable Intelligent Surface Aided Constant-Envelope Wireless Power Transfer," in IEEE Transactions on Signal Processing, vol. 69, pp. 1347-1361, 2021, doi: 10.1109/TSP.2021.3056906.
194 Z. Chu, Z. Zhu, F. Zhou, M. Zhang and N. Al-Dhahir, "Intelligent Reflecting Surface Assisted Wireless Powered Sensor Networks for Internet of Things," in IEEE Transactions on Communications, vol. 69, no. 7, pp. 4877-4889, July 2021, doi: 10.1109/TCOMM.2021.3074539.
195 B. Lyu, P. Ramezani, D. T. Hoang, S. Gong, Z. Yang and A. Jamalipour, "Optimized Energy and Information Relaying in Self-Sustainable IRS-Empowered WPCN," in IEEE Transactions on Communications, vol. 69, no. 1, pp. 619-633, Jan. 2021, doi: 10.1109/TCOMM.2020.3028875.
196 W. Shi, X. Zhou, L. Jia, Y. Wu, F. Shu and J. Wang, "Enhanced Secure Wireless Information and Power Transfer via Intelligent Reflecting Surface," in IEEE Communications Letters, vol. 25, no. 4, pp. 1084-1088, April 2021, doi: 10.1109/LCOMM.2020.3043475.
197 B. H. Fong, J. S. Colburn, J. J. Ottusch, J. L. Visher and D. F. Sievenpiper, "Scalar and Tensor Holographic Artificial Impedance Surfaces," IEEE Transactions on Antennas and Propagation, vol. 58, no. 10, pp. 3212-3221, Oct. 2010.
198 C. Huang et al., "Holographic MIMO Surfaces for 6G Wireless Networks: Opportunities, Challenges, and Trends," IEEE Wireless Communications, vol. 27, no. 5, pp. 118-125, October 2020.
199 K. Onizuka, H. Kawaguchi, M. Takamiya, T. Kuroda and T. Sakurai, "Chip-to-Chip Inductive Wireless Power Transmission System for SiP Applications," IEEE Custom Integrated Circuits Conference 2006, pp. 575-578, doi: 10.1109/CICC.2006.320994.
200 H. Dang-ba and G. Byun, "A Sub-THz Wireless Power Transfer for Non-Contact Wafer-Level Testing," Electronics, vol. 9, no. 8, p. 1210, Jul. 2020.
201 N. Shinohara, "Trends in Wireless Power Transfer: WPT Technology for Energy Harvesting, Mllimeter-Wave/THz Rectennas, MIMO-WPT, and Advances in Near-Field WPT Applications," IEEE Microwave Magazine, vol. 22, no. 1, pp. 46-59, Jan. 2021, doi: 10.1109/MMM.2020.3027935.

AUTHOR INFORMATION:

Jiafeng Zhou received a B.Sc. degree in Radio Physics from Nanjing University, Nanjing, China, in 1997, and a Ph.D. degree from the University of Birmingham, Birmingham, U.K., in 2004. His doctoral research concerned high-temperature superconductor microwave filters.

From July 1997, for two and a half years he was with the National Meteorological Satellite Centre of China, Beijing, China, where he was involved with the development of communication systems for Chinese geostationary meteorological satellites. From August 2004 to April 2006, he was a Research Fellow with the University of Birmingham, where his research concerned phased arrays for reflector observing systems. Then he moved to the Department of Electronic and Electrical Engineering, University of Bristol, Bristol, U.K until August 2013. His research in Bristol was on the development of highly efficient and linear amplifiers. He is now with the Department of Electrical Engineering and Electronics, University of Liverpool, Liverpool, UK. His current research interests include microwave and radio frequency components and devices, metamaterials, electromagnetic energy harvesting and wireless power transfer.

Pei Zhang was born in Yangzhou, China, in 1992. He received the B. E. Degree in radio wave propagation and antenna from Xidian University, Xi'an, China, in 2017. He received the Ph.D. degree in electromagnetic fields and microwave technology at Xidian University, Xi'an, China. He is currently an engineer with Nanjing Research Institute of Electronic Engineering.
His research interests include wireless power transfer, wireless energy harvesting, metasurfaces, and electromagnetic field simulation and optimization.

Jiaqi Han (M'20) was born in Henan, China, in 1991. He received the B.E. degree in electronic and information engineering from Henan Normal University, Xinxiang, China, in 2014, and the Ph.D. degree in electromagnetic fields and microwave technology from Xidian University, Xi'an, China, in 2019.
He is currently a Post-Doctoral Fellow with the School of Electronic Engineering, Xidian University. His research interests include the design of programmable metasurfaces and their applications on wireless power transfer and computational imaging.

Long Li (M'06-SM'11) received the B. E. and Ph. D. degrees in electromagnetic fields and microwave technology from Xidian University, Xi'an, China, in 1998 and 2005, respectively.
He was a Senior Research Associate in the Wireless

Communications Research Center, City University of Hong Kong in 2006. He received the Japan Society for Promotion of Science (JSPS) Postdoctoral Fellowship and visited Tohoku University, Sendai, Japan, as a JSPS Fellow from 2006 to 2008. He was a Senior Visiting Scholar in the Pennsylvania State University, USA, in 2014. He is currently a Professor in the School of Electronic Engineering, Xidian University. Prof. Li is the Director of Key Laboratory of High-Speed Circuit Design and EMC, Ministry of Education, China, and the Dean of Hai-Tang No.9 Academy of Xidian University. His research interests include metamaterials/metasurfaces, antennas and microwave devices, field- circuit collaborative design and EMC, wireless power transfer and harvesting technology, OAM vortex waves. He has authored or co-authored over 120 papers in journals and held more than 20 patents.

Prof. Li received Nomination Award of National Excellent Doctoral Dissertation of China in 2007. He won the Best Paper Award in the International Symposium on Antennas and Propagation in 2008. He received the Program for New Century Excellent Talents in University of the Ministry of Education of China in 2010. He won the First Prize of Awards for Scientific Research Results offered by Shaanxi Provincial Department of Education, China, in 2013. He received the IEEE APS Raj Mittra Travel Grant Senior Researcher Award in 2015. Prof. Li received Shaanxi Youth Science and Technology Award in 2016, and Distinguished Young Scholars Foundation of Shaanxi Province of China, in 2019. Prof. Li was awarded a Chang-Jiang Scholars Distinguished Professor by the Ministry of Education, China, in 2021. Prof. Li is the Vice-President of MTT-Chapter in IEEE Xi'an Section. He is a TPC Co-Chair of APCAP2017 and a General Co-Chair of AWPT2019. He serves as an Associate Editor of ACES Journal and Guest Editor of IEEE J-ERM Special Issue

Yi Huang (Fellow, IEEE) received BSc in Physics (Wuhan, China) in 1984, MSc (Eng) in Microwave Engineering (Nanjing, China) in 1987, and DPhil in Communications from the University of Oxford, UK in 1994.

He has been conducting research in the areas of antennas, wireless communications, applied electromagnetics, radar, and EMC since 1987. More recently, he is focused on mobile antennas, wireless energy harvesting, and power transfer. His experience includes 3 years spent with NRIET (China) as a Radar Engineer and various periods with the Universities of Birmingham, Oxford, and Essex in the UK as a member of research staff. He worked as a Research Fellow at British Telecom Labs in 1994 and then joined the Department of Electrical Engineering & Electronics, the University of Liverpool, UK as a Faculty in 1995, where he is now a full Professor in Wireless Engineering, the Head of High-Frequency Engineering Group and Deputy Head of Department.

Prof Huang has published over 500 refereed papers in leading international journals and conference proceedings and authored four books, including Antennas: from Theory to Practice (John Wiley, 2008, 2021). He has received many patents, research grants from research councils, government agencies, charities, EU, and industry, and is a recipient of over 10 awards (e.g. BAE Systems Chairman's Award 2017, IET, and Best Paper Awards). He has served on a number of national and international technical committees and been an Editor, Associate Editor, or Guest Editor of five international journals. In addition, he has been a keynote/invited speaker and organiser of many conferences and workshops (e.g. IEEE iWAT2010, LAPC2012, and EuCAP2018). He is at present the Editor-in-Chief of Wireless Engineering and Technology, Associate Editor of IEEE Antennas and Wireless Propagation Letters, UK and Ireland Rep to European Association of Antenna and Propagation (EurAAP, 2016-2020), a Fellow of IET, and a Fellow of IEEE.